

Can Auxiliary Indicators Improve COVID-19 Forecasting and Hotspot Prediction?

Daniel J. McDonald^{a,1}, Jacob Bien^{b,2}, Alden Green^{c,2}, Addison J. Hu^{c,d,2}, Nat DeFries^d, Sangwon Hyun^b, Natalia L. Oliveira^{c,d}, James Sharpnack^e, Jingjing Tang^f, Robert Tibshirani^{g,h}, Valérie Ventura^c, Larry Wasserman^{c,d}, and Ryan J. Tibshirani^{c,d}

^aDepartment of Statistics, University of British Columbia

^bDepartment of Data Sciences and Operations, University of Southern California

^cDepartment of Statistics & Data Science, Carnegie Mellon University

^dMachine Learning Department, Carnegie Mellon University

^eDepartment of Statistics, University of California, Davis

^fComputational Biology Department, Carnegie Mellon University

^gDepartment of Statistics, Stanford University

^hDepartment of Biomedical Data Science, Stanford University

June 22, 2021

Abstract

Reliable, short-term forecasts of traditional public health reporting streams (such as cases, hospitalizations, and deaths) are a key ingredient in effective public health decision-making during a pandemic. Since April 2020, our research group has worked with data partners to collect, curate, and make publicly available numerous real-time COVID-19 indicators, providing multiple views of pandemic activity. This paper studies the utility of these indicators from a forecasting perspective. We focus on five indicators, derived from medical insurance claims data, web search queries, and online survey responses. For each indicator, we ask whether its inclusion in a simple model leads to improved predictive accuracy relative to a similar model excluding it. We consider both probabilistic forecasting of confirmed COVID-19 case rates and binary prediction of case “hotspots”. Since the values of indicators (and case rates) are commonly revised over time, we take special care to ensure that the data provided to a forecaster is the version that would have been available at the time the forecast was made. Our analysis shows that consistent but modest gains in predictive accuracy are obtained by using these indicators, and furthermore, these gains are related to periods in which the auxiliary indicators behave as “leading indicators” of case rates.

Keywords: COVID-19 | forecasting | hotspot prediction | time series | digital surveillance

¹To whom correspondence should be addressed. E-mail: daniel@stat.ubc.ca

²J.B., A.G., and A.J.H. contributed equally to this work.

Tracking and forecasting indicators from public health reporting streams—such as confirmed cases and deaths in the COVID-19 pandemic—is crucial for understanding disease spread, formulating public policy responses, and anticipating future public health resource needs. In a companion paper, we describe our research group’s (Delphi’s) efforts in curating and maintaining a database of real-time indicators that track COVID-19 activity and other relevant phenomena. The signals (a term we use synonymously with “indicators”) in this database are accessible through the COVIDcast API [1], with associated R [2] and Python [3] packages for convenient data fetching and processing tools. In the current paper, we aim to quantify the utility provided by a core set of these indicators for two fundamental prediction tasks: probabilistic forecasting of COVID-19 case rates and prediction of future COVID-19 case hotspots (defined by the event that a relative increase in COVID-19 cases exceeds a certain threshold).

At the outset, we should be clear that our intent in this paper is *not* to provide an authoritative take on cutting-edge COVID-19 forecasting methods. Instead, our purpose here is to provide a rigorous, quantitative assessment of the utility that several auxiliary indicators—such as those derived from internet surveys or medical insurance claims—provide in tasks that involve predicting future trends in confirmed COVID-19 cases. To assess such utility in as simple terms as possible, we center our study in the framework of a basic autoregressive model (in which COVID cases in the near future are predicted from a linear combination of COVID cases in the near past), and ask whether the inclusion of an auxiliary indicator as an additional feature in such a model improves its predictions.

While forecasting carries a rich literature that offers a wide range of techniques, see e.g., [4], we purposely constrain ourselves to very simple models, avoiding common enhancements such as order selection, correction of outliers/anomalies in the data, and inclusion of regularization or nonlinearities. That said, analyses of forecasts submitted to the COVID-19 Forecast Hub [5] by a large community of modelers have shown that simple, robust models have consistently been among the best-performing over the pandemic [6], including time series models similar to those we consider in what follows.

In our companion paper, we analyze correlations between various indicators and COVID case rates. These correlations are natural summaries of the contemporaneous association between an indicator and COVID cases, but they fall short of delivering a satisfactory answer to the question that motivates the current article: is the information contained in an indicator demonstrably useful for the prediction tasks we care about? For such a question, lagged correlations (e.g., measuring the correlation between an indicator and COVID case rates several days in the future) move us in the right direction, but still do not move us all the way there. The question about *utility for prediction* is focused on a much higher standard than simply asking about correlations; to be useful in forecast or hotspot models, an indicator must provide relevant information that is not otherwise contained in past values of the case rate series itself. We will assess this in the most direct way possible: by inspecting the difference in predictive performance of simple autoregressive models trained with and without access to past values of a particular indicator.

There is another, more subtle issue in evaluating predictive utility that deserves explicit mention, as it will play a key role in our analysis. Signals computed from surveillance streams will often be subject to latency and/or revision. For example, a signal based on aggregated medical insurance claims may be available after just a few days, but it can then be substantially revised over the next several weeks as additional claims are submitted and/or processed late. Correlations between such a signal and case rates calculated “after the fact” (i.e., computed retrospectively, using the finalized values of this signal) will not deliver an honest answer to the question of whether this signal would have been useful in real time. Instead, we build predictive models using only the data that would have been available *as of* the prediction date, and compare the ensuing predictions in terms of accuracy. To do so, we leverage Delphi’s `evalcast` R package [7], which plugs into the COVIDcast API’s data versioning system, and facilitates honest backtesting.

Finally, it is worth noting that examining the importance of additional features for prediction is a core question in inferential statistics and econometrics, with work dating back to at least [8]. Still today, drawing rigorous inference based on predictions, without (or with lean) assumptions, is an active field of research from both the applied and theoretical angles; see, e.g., [9–18]. Our take on this problem is in line with much of this literature; however, in order to avoid making any explicit assumptions, we do not attempt to make formal significance statements, and instead, broadly examine the stability of our conclusions with respect to numerous modes of analysis.

1 Methods

1.1 Signals and Locations

We consider prediction of future COVID-19 case rates or case hotspots (to be defined precisely shortly). By case rate, we mean the case count per 100,000 people (the standard in epidemiology). We use reported case data aggregated by JHU CSSE [19], which, like the auxiliary indicators that we use to supplement the basic autoregressive models, is accessible through the COVIDcast API [1].

The indicators we focus on provide information not generally available from standard public health reporting. Among the many auxiliary indicators collected in the API, we study the following five:

- Change Healthcare COVID-like illness (CHNG-CLI): The percentage of outpatient visits that are primarily about COVID-related symptoms, based on de-identified Change Healthcare claims data.
- Change Healthcare COVID (CHNG-COVID): The percentage of outpatient visits with confirmed COVID-19, based on the same claims data.
- COVID Trends and Impact Survey COVID-like illness in the community (CTIS-CLI-in-community): The estimated percentage of the population who know someone in their local community who is sick, based on Delphi’s COVID Trends and Impact Survey, in partnership with Facebook.
- Doctor Visits COVID-like illness (DV-CLI): The same as CHNG-CLI, but computed based on de-identified medical insurance claims from other health systems partners.
- Google search trends for anosmia and ageusia (Google-AA): A measure of Google search volume for queries that relate to anosmia or ageusia (loss of smell or taste), based on Google’s COVID-19 Search Trends data set.

In short, we choose these indicators because, conceptually speaking, they measure aspects of an individual’s disease progression that would plausibly precede the occurrence of (at worst, co-occur with) the report of a positive COVID-19 test, through standard public health reporting streams.

For more details on the five indicators (including how these are precisely computed from the underlying data streams) we refer to https://cmu-delphi.github.io/delphi-epidata/api/covidcast_signals.html, which documents all of the signals in the COVIDcast API, and our companion paper on the API and database. For CTIS in particular, we refer to our companion paper on this survey. For the Google COVID-19 Search Trends data set, see [20]; see also [21, 22] for a justification of the relevance of anosmia or ageusia to COVID-19 infection.

As for geographic resolution, we consider the prediction of COVID-19 case rates and hotspots aggregated at the level of an individual *hospital referral region* (HRR). HRRs correspond to groups of counties in the United States within the same hospital referral system. The Dartmouth Atlas of Healthcare Policy [23], defines these 306 regions based on a number of characteristics. They are contiguous regions such that most of the hospital services for the underlying population are performed by hospitals within the region. Each HRR also contains at least one city where major procedures (cardiovascular or neurological) are performed. The smallest HRR has a population of about 125,000. While some are quite large (such as the one containing Los Angeles, which has more than 10 million people), generally HRRs are much more homogenous in size than the (approximately) 3200 counties, and they serve as a nice middle ground in between counties and states.

HRRs, by their definition, would be most relevant for forecasting hospital demand. We have chosen to focus on cases (forecasting and predicting hotspots) at the HRR level because the indicators considered should be more useful in predicting case activity rather than hospital demand, as the former is intuitively more contemporaneous to the events that are measured by the given five indicators. Predicting case rates (and hotspots) at the HRR level is still a reasonable goal in its own right; and moreover, it could be used to feed predicted case information into downstream hospitalization models.

1.2 Vintage Training Data

In this paper, all models are fit with “vintage” training data. This means that for a given prediction date, say, September 28, 2020, we train models using data that would have been available to us *as of* September

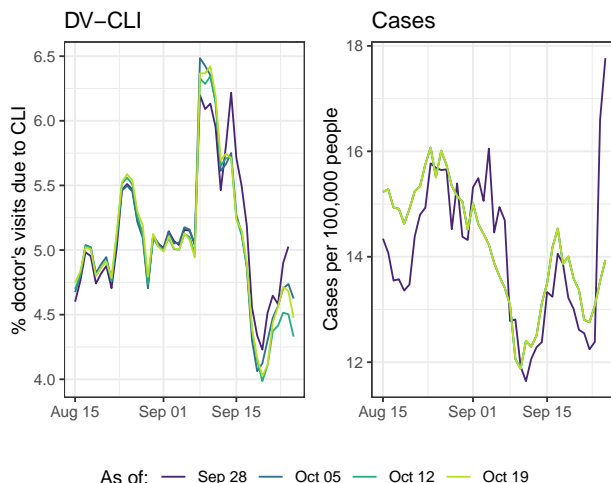


Figure 1: Revision behavior for two indicators in the HRR containing Charlotte, North Carolina. Each colored line corresponds to the data as reported on a particular date (*as of* dates varying from September 28 through October 19). The left panel shows the DV-CLI signal, which was regularly revised throughout the period, though the effects fade as we look further back in time. In contrast, the right panel shows case rates reported by JHU CSSE (smoothed with a 7-day trailing average), which remain “as reported” on September 28, with a spike towards the end of this period, until a major correction is made on October 19, which brings this down and affects all prior data as well.

28 (imagine that we can “rewind” the clock to September 28 and query the COVIDcast API to get the latest data it would have had available at that point in time.) This is possible because of the COVIDcast API’s comprehensive data versioning system (described in more detail in our companion paper). We also use the `evalcast` R package [7], which streamlines the process of training arbitrary prediction models over a sequence of prediction dates, by constructing the proper sequence of vintage training data sets.

Vintage training data means different things, in practice, for different signals. The three signals based on medical claims, CHNG-CLI, CHNG-COVID, and DV-CLI, are typically 3-5 days latent, and subject to a considerable but regular degree of revision or “backfill” after their initial publication date. The survey-based signal, CTIS-CLI-in-community, is 2 days latent, and rarely undergoes any revision at all. The target variable itself, reported COVID-19 case rates, is 1 day latent, and exhibits frequent, unpredictable revisions after initial publication. Compared to the pattern of revisions in the medical claims signals, which are much more systematic in nature, revisions in case reports can be highly erratic. Big spikes or other anomalies can occur in the data as reporting backlogs are cleared, changes in case definitions are made, etc. Groups like JHU CSSE then work tirelessly to correct such anomalies after first publication (e.g., they will attempt to back-distribute a spike when a reporting backlog is cleared, by working with a local authority to figure out how this should best be done), which can result in very nontrivial revisions. See Figure 1 for an example.

Lastly, our treatment of the Google-AA signal is different from the rest. Because Google’s team did not start publishing this signal until early September, 2020, we do not have true vintage data before then. Furthermore, the latency of the signal was always at least one week through 2020. However, this signal is never revised after initial publication (confirmed via personal communication with the Google team that produces this signal) and furthermore the latency of the signal is not an unavoidable property of the data type, so we simply use finalized signal values, with zero latency, in our analysis.

1.3 Analysis Tasks

To fix notation, let $Y_{\ell,t}$ denote the 7-day trailing average of COVID-19 case incidence rates in location (HRR) ℓ and at time (day) t . To be clear, this is the number of new daily reported cases per 100,000 people, averaged over the 7-day period $t-6, \dots, t$. The first task we consider—*forecasting*—is to predict $Y_{\ell,t+a}$ for each “ahead” value $a = 7, \dots, 21$. The second task—*hotspot prediction*—is to predict a binary variable defined in terms of

Table 1: Summary of forecasting and hotspot prediction tasks considered in this paper.

	Forecasting	Hotspot prediction
Response variable	$Y_{\ell,t}$ (7-day trailing average of COVID-19 case incidence rates, per location ℓ and time t)	$Z_{\ell,t} = \mathbf{1}(Y_{\ell,t} \geq 1.25 \cdot Y_{\ell,t-7})$ (indicator that $Y_{\ell,t}$ grows by more than 25% relative to the preceding week)
Geographic resolution	Hospital referral region (HRR)	Hospital referral region (HRR)
Forecast period	June 9–December 31, 2020	June 16–December 31, 2020
Model type	Quantile regression	Logistic regression
Evaluation metric	Weighted interval score (WIS)	Area under curve (AUC)

the relative change of $Y_{\ell,t+a}$ (relative to its value one week prior, $Y_{\ell,t+a-7}$), again for each $a = 7, \dots, 21$.

Why do we define the response variables via 7-day averaging? The short answer is robustness: averaging stabilizes the case time series, and accounts for uninteresting artifacts like day-of-the-week effects in the series. Note that we can also equivalently view this (equivalent up to a constant factor) as predicting the HRR-level case incidence rate *summed* over some 7-day period in the future, and predicting a binary variable derived from this.

In what follows, we cover more details on our two analysis tasks. Table 1 presents a summary.

Dynamic Re-Training For each prediction date t , we use a 21-day trailing window of data to train our forecast or hotspot prediction models (so, e.g., the trained models will differ from those at prediction date $t - 1$). This is done to account for (potential) nonstationarity. For simplicity, the forecasting and hotspot prediction models are always trained on data across all HRRs (i.e., the coefficients in the models do not account for location-specific effects).

Prediction Period In our analysis, we let the prediction date t run over each day in between early/mid June and December 31, 2020. The precise start date differs for forecasting and hotspots prediction; for each task it was chosen to be the earliest date at which the data needed to train all models was available, which ends up being (per our setup, with 21 days of training data and lagged values of signals for features, as we will detail shortly) June 9, 2020 for forecasting, and June 16, 2020 for hotspot prediction. (The bottleneck here is the CTIS-CLI-in-community signal, which does not exist before early April 2020, when the survey was first launched). The end date was chosen again with a consideration to align both tasks as best as possible, and because few hotspots exist post December 31, 2020, due to the general and gradual decline of the pandemic in 2021.

Forecasting Models Recall $Y_{\ell,t}$ denotes the 7-day trailing average of COVID-19 case incidence rates in location ℓ and at time t . Separately for each $a = 7, \dots, 21$, to predict $Y_{\ell,t+a}$ for ahead value a , we consider a simple probabilistic forecasting model of the form:

$$\text{Quantile}_{\tau}(Y_{\ell,t+a} \mid Y_{\ell,s}, s \leq t) = \alpha^{a,\tau} + \sum_{j=0}^2 \beta_j^{a,\tau} Y_{\ell,t-7j}. \quad (1)$$

This model uses current case rates, and the case rates 7 and 14 days ago, in order to predict (the quantiles of) case rates in the future. We consider a total of 7 quantile levels (chosen in accordance with the county-level quantile levels suggested by the COVID-19 Forecast Hub),

$$\tau \in \{0.025, 0.1, 0.25, 0.5, 0.75, 0.9, 0.975\}. \quad (2)$$

We fit (1) using *quantile regression* [24–26] separately for each τ , using data from all 306 HRRs, and within each HRR, using the most recent 21 days of training data. This gives us 6,426 training samples for each quantile regression problem.

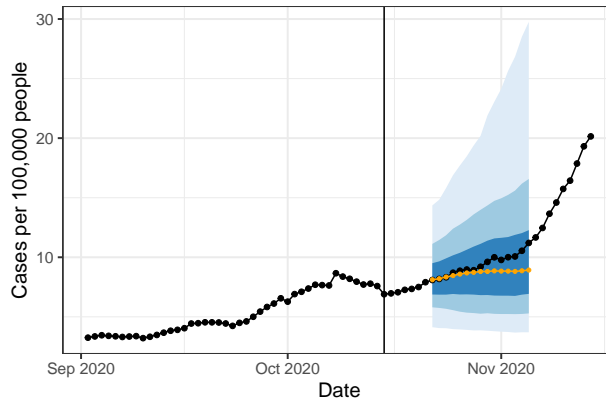


Figure 2: Forecast for the HRR containing New York City from an autoregressive model made on October 15 (vertical line). The fan displays 50%, 80% and 95% intervals while the orange curve shows the median forecast. The black curve shows “finalized” data, as reported in May 2021.

In addition to this pure autoregressive model, we also consider five probabilistic forecasting models of the form:

$$\text{Quantile}_\tau(Y_{\ell,t+a} \mid Y_{\ell,s}, X_{\ell,s}, s \leq t) = \alpha^{a,\tau} + \sum_{j=0}^2 \beta_j^{a,\tau} Y_{\ell,t-\tau j} + \sum_{j=0}^2 \gamma_j^{a,\tau} X_{\ell,t-\tau j}, \quad (3)$$

where $X_{\ell,t}$ denotes any one of the five auxiliary indicators—CHNG-CLI, CHNG-COVID, CTIS-CLI-in-community, DV-CLI, or Google-AA—at location ℓ and time t . Note that we apply the same lags (current value, along with the values 7 and 14 days ago) for the auxiliary indicators as we do for the case rates. Training then proceeds just as before: we use the same 7 quantile levels in (2), and fit quantile regression separately for each level τ , using data from all 306 HRRs and a trailing window of 21 days of training data.

At prediction time, in order to avoid crossing violations (that is, for two levels $\tau' > \tau$, the predicted quantile at level τ exceeds the predicted quantile at level τ'), we apply a simple post-hoc sorting. See Figure 2 for an example forecast.

Hotspot Prediction Models Define the binary indicator:

$$Z_{\ell,t} = \mathbf{1}(Y_{\ell,t}^\Delta \geq 0.25),$$

where we use the notation $Y_{\ell,t}^\Delta = (Y_{\ell,t} - Y_{\ell,t-7}) / (Y_{\ell,t-7})$. In other words, $Z_{\ell,t} = 1$ if the number of newly reported cases over the past 7 days has increased by at least 25% compared to the preceding week. When this occurs, we say location ℓ is a *hotspot* at time t . Empirically, this rule labels about 27% of location-time pairs as hotspots, during the prediction period (June 16–December 31, 2020).

We treat hotspot prediction as a binary classification problem and use a setup altogether quite similar to the forecasting setup described previously. Separately for each $a = 7, \dots, 21$, to predict $Z_{\ell,t+a}$, we consider a simple logistic model:

$$\text{logit}(\mathbb{P}(Z_{\ell,t+a} = 1 \mid Y_{\ell,s}, s \leq t)) = \alpha^{a,\tau} + \sum_{j=0}^2 \beta_j^{a,\tau} Y_{\ell,t-\tau j}^\Delta, \quad (4)$$

where $\text{logit}(p) = \log(p/(1-p))$, the log-odds of p .

In addition to this pure autoregressive model, we also consider five logistic models of the form:

$$\text{logit}(\mathbb{P}(Z_{\ell,t+a} = 1 \mid Y_{\ell,s}, X_{\ell,s}, s \leq t)) = \alpha^{a,\tau} + \sum_{j=0}^2 \beta_j^{a,\tau} Y_{\ell,t-\tau j}^\Delta + \sum_{j=0}^2 \gamma_j^{a,\tau} X_{\ell,t-\tau j}^\Delta, \quad (5)$$

where we use $X_{\ell,t}^{\Delta} = (X_{\ell,t} - X_{\ell,t-7}) / (X_{\ell,t-7})$, and again $X_{\ell,t}$ stands for any of the five auxiliary indicators at location ℓ and time t . We fit the above models, (4), (5), using logistic regression, pooling all 306 HRRs and using a 21-day trailing window for the training data.

An important detail is that in hotspot prediction we remove all data from training and evaluation where, on average, fewer than 30 cases (this refers to a count, not a rate) are observed over the preceding 7 days. This avoids having to make arbitrary calls for a hotspot (or lack thereof) based on small counts.

1.4 Evaluation Metrics

For forecasting, we evaluate the probabilistic forecasts produced by the quantile models in (1) and (3) using *weighted interval score* (WIS), a quantile-based scoring rule; see e.g., [27]. WIS is a proper score, which means that its expectation is minimized by the population quantiles of the target variable. The use of WIS in COVID-19 forecast scoring is discussed in [28]; WIS is also the main evaluation metric used in the COVID-19 Forecast Hub.

WIS is typically defined for quantile-based forecasts where the quantile levels are symmetric around 0.5. This is the case for our choice in (2). Let F be a forecaster comprised of predicted quantiles q_{τ} parametrized by a quantile level τ . In the case of symmetric quantile levels, this is equivalent to a collection of central prediction intervals $(\ell_{\alpha}, u_{\alpha})$, parametrized by an exclusion probability α . The WIS of the forecaster F , evaluated at the target variable Y , is defined by:

$$\text{WIS}(F, Y) = \sum_{\alpha} \left\{ \alpha(u_{\alpha} - \ell_{\alpha}) + 2 \cdot \text{dist}(Y, [\ell_{\alpha}, u_{\alpha}]) \right\}, \quad (6)$$

where $\text{dist}(a, S)$ is the distance between a point a and set S (the smallest distance between a and an element of S). Note that, corresponding to (2), the exclusion probabilities are $\alpha \in \{0.05, 0.2, 0.5, 1\}$, resulting in 4 terms in the above sum. By straightforward algebra, it is not hard to see WIS has an alternative representation in terms of the predicted quantiles themselves:

$$\text{WIS}(F, Y) = 2 \sum_{\tau} \phi_{\tau}(Y - q_{\tau}), \quad (7)$$

where $\phi_{\tau}(x) = \tau|x|$ for $x \geq 0$ and $\phi_{\tau}(x) = (1 - \tau)|x|$ for $x < 0$, which is often called the “tilted absolute” loss. While (7) is more general (it can accommodate asymmetric quantile levels), the first form in (6) is typically preferred in presentation, as the score nicely decouples into a “sharpness” component (first term in each summand) and an “under/overprediction” component (second term in each summand). But the second form given in (7) is especially noteworthy in our current study because it reveals WIS to be the same as the quantile regression loss that we use to train our forecasting models (i.e., we fit by optimizing WIS averaged over the training data).

For hotspot prediction, we evaluate the probabilistic classifiers produced by the logistic models in (4) and (5) using the area under the curve (AUC) of their true positive versus false positive rate curve (which is traced out by varying the discrimination threshold).

The primary aggregation scheme that we will use in model evaluation and comparisons will be to average WIS per forecaster at ahead value a over all forecast dates t and locations ℓ ; and similarly, to compute AUC per classifier at ahead value a over all forecast dates t and locations ℓ .

1.5 Other Considerations

Missing Data Imputation Over the prediction period, all auxiliary indicators are available (in the proper vintage sense) for all locations and prediction times, except for the Google-AA signal, which is only observed for an average of 105 (of 306) HRRs. Such missingness occurs because the COVID-19 search trends data is constructed using differential privacy methods [29], and a missing signal value means that the level of noise added in the differential privacy mechanism is high compared to the underlying search count. In other words, values of the Google-AA signal are clearly *not* missing at random. It seems most appropriate to impute missing values by zero, and this is what we do in our analysis.

Backfill and Nowcasting As described previously, the auxiliary indicators defined in terms of medical claims (CHNG-CLI, CHNG-COVID, and DV-CLI) undergo a significant and systematic pattern of revision, or “backfill”, after their initial publication. Given their somewhat statistically-regular backfill profiles, it would be reasonable to attempt to estimate their finalized values based on vintage data—a problem we refer to as *nowcasting*—as a pre-processing step before using them as features in the models in (3) and (5). Nowcasting is itself a highly nontrivial modeling problem, and we do not attempt it in this paper (it is a topic of ongoing work in our research group), but we note that nowcasting would likely improve the performance of the models involving claims-based signals in particular.

Spatial Heterogeneity Some signals have a significant amount of spatial heterogeneity, by which we mean their values across different geographic locations are not comparable. This is the case for the Google-AA signal (due to the way in which the underlying search trends time series is self-normalized, see [20]) and the claims-based signals (due to market-share differences, and/or differences in health-seeking behavior). Such spatial heterogeneity likely hurts the performance of the predictive models that rely on these signals, because we train the models on data pooled over all locations. In the current paper, we do not attempt to address this issue (it is again a topic of ongoing work in our group), and we simply note that location-specific effects (or pre-processing to remove spatial bias) would likely improve the performance of the models involving Google-AA and the claims-based indicators.

2 Results

Here, and in what follows, we will use “AR” to refer to the pure autoregressive model both in forecasting, (1), and in hotspot prediction, (4) (the reference to the prediction task should always be clear from the context). We will also use the name of an auxiliary indicator—namely “CHNG-CLI”, “CHNG-COVID”, “CTIS-CLI-in-community”, “DV-CLI”, or “Google-AA”—interchangeably with the model in forecasting, (3), or hotspot prediction, (5), that uses this particular indicator as a feature (the meaning should be clear from the context). So, for example, the CHNG-CLI model in forecasting is the one in (3) that sets $X_{\ell,t}$ to be the value of the CHNG-CLI indicator at location ℓ and time t . Finally, we use the term “indicator model” to refer to any one of the ten models of the form (3) or (5) (five from each of the forecasting and hotspot prediction tasks).

We begin with a summary of the high-level conclusions.

- Stratifying predictions by the ahead value ($a = 7, \dots, 21$), and aggregating results over the prediction period (early June through end of December 2020), we find that each of the indicator models generally gives a boost in predictive accuracy over the AR model, in both the forecasting and hotspot prediction tasks. The gains in accuracy generally attenuate as the ahead value grows.
- In the same aggregate view, CHNG-COVID and DV-CLI offer the biggest gains in both forecasting and hotspot prediction. CHNG-CLI is inconsistent: it provides a big gain in hotspot prediction, but little gain in forecasting (it seems to be hurt by a notable lack of robustness, due to backfill). CTIS-CLI-in-community and Google-AA each provide decent gains in forecasting and hotspot prediction. The former’s performance in forecasting is notable in that it clearly improves on AR even at the largest ahead values.
- In a more detailed analysis of forecasting performance, we find that the indicator models tend to be better than AR when case rates are flat or decreasing (most notable in CHNG-COVID and CTIS-CLI-in-community), but they are worse than AR when case rates are increasing (this is most notable in CHNG-CLI and DV-CLI). More rarely does an indicator model tend to beat AR when case rates are increasing, but there appears to be some evidence of this for the Google-AA model.
- In this same analysis, when an indicator model performs better than AR in a decreasing period, this tends to co-occur with instances in which the indicator “leads” case rates (meaning, roughly, on a short-time scale in a given location, its behavior mimics that of future case rates). On the other hand, if an indicator model does better in periods of increase, or worse in periods of increase or decrease, its performance is not as related to leadingness.

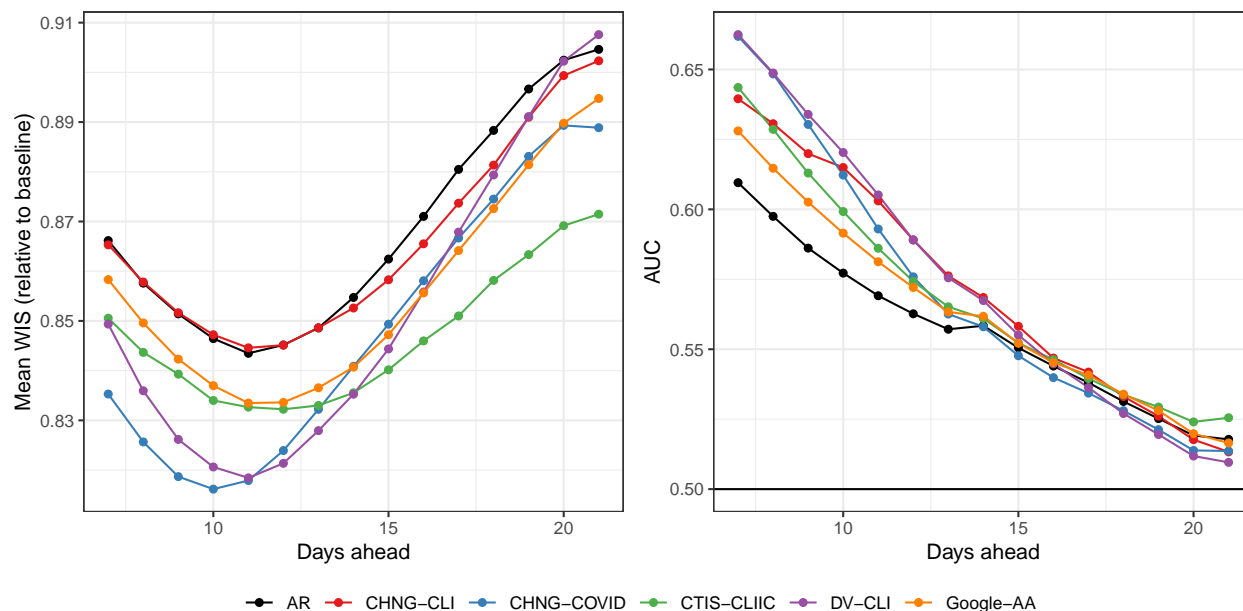


Figure 3: Main results for both tasks. Left: average WIS for each forecast model, over all forecast dates and all HRRs, divided by the average WIS achieved by a baseline model (a probabilistic version of the flat-line forecaster). Right: area under the curve for each hotspot prediction model, calculated over all prediction dates and all HRRs. Here and in all figures we abbreviate CTIS-CLI-in-community by CTIS-CLIIC.

Finally, to quantify the importance of training and making predictions using proper vintage data, we ran a parallel set of forecasting and hotspot prediction experiments using finalized data. The results, given in the supplement, show that training and making predictions on finalized data can result in overly optimistic estimates of true test-time performance (up to 10% better in terms of average WIS or AUC). Furthermore, since indicators can have greatly different backfill profiles, the use of finalized data in retrospective evaluations changes the relative ranking of models. For example, CHNG-CLI and DV-CLI, when trained on finalized data, perform very similarly in forecasting. This makes sense since they are both claims-based indicators that are supposedly measuring the same thing. However, DV-CLI outperforms CHNG-CLI on vintage data, reflecting its has a less severe backfill profile.

Code to reproduce all results (which uses the `evalcast` R package) can be found at <https://github.com/cmu-delphi/covidcast-pnas/tree/main/forecast/code>.

2.1 Aggregate Results by Ahead Value

Figure 3 (left panel) displays evaluation results for forecasting, stratified by ahead value and averaged over all HRRs and forecast dates. Shown is the average WIS for each forecast model divided by that from a baseline model, which is basically a flat-line forecaster (its median forecast for $Y_{\ell,t+a}$ is always $Y_{\ell,t}$, with predicted quantiles defined around this based on historical variation). This is the same baseline model as in the COVID-19 Forecast Hub. Here, we use the baseline model in order to scale mean WIS so that it gets put on an interpretable, unitless scale. In the figure, we can see that all curves are below 1, which means (smaller WIS is better) that all of the models, including AR, outperform the baseline on average over the forecasting period. On the other hand, the models deliver at best an improvement of about 20% in average WIS over the baseline model, with this gap narrowing to about 10% at the largest ahead values, illustrating the difficulty of the forecasting problem.

We can also see from the figure that CHNG-COVID and DV-CLI offer the biggest gains over AR at small ahead values, followed by CTIS-CLI-in-community and Google-AA, with the former providing the biggest gains at large ahead values. The CHNG-CLI model performs basically the same as AR. This is likely due to the fact that CHNG-CLI suffers from volatility due to backfill. The evidence for this explanation is twofold: (1) the CHNG-CLI model benefits from a more robust method of aggregating WIS (geometric mean; shown

in the supplement); and (2) when we train and make predictions on finalized data, it handily beats AR, on par with the best-performing models (also shown in the supplement).

Figure 3 (right panel) displays the results for hotspot prediction, again stratified by ahead value and averaged over all HRRs and prediction dates. We can see many similarities to the forecasting results (now larger AUC is better). For example, CHNG-COVID and DV-CLI offer the biggest improvement over AR, and all models, including AR, degrade in performance towards the baseline (in this context, a classifier based on random guessing, which achieves an AUC of 0.5) as the ahead values grow, illustrating the difficulty of the hotspot prediction problem. A clear difference, however, is that the CHNG-CLI model performs quite well in hotspot prediction, close to the best-performing indicator models for many of the ahead values. This may be because volatility in the CHNG-CLI indicator plays less of a role in the associated logistic model’s predicted probabilities (in general, a sigmoid function can absorb a lot of the variability in its input).

2.2 Implicit Regularization Hypothesis

One might ask if the benefits we observe in forecasting and hotspot prediction have anything to do with the actual indicator themselves. A plausible alternative explanation is that the indicators are simply providing *implicit regularization* on top of the basic AR model, in the same way any noise variable might, when we include them as lagged features in (3) and (5).

To test this hypothesis, we reran all of the prediction experiments but with $X_{\ell,t}$ in the each indicator models replaced with suitable random noise (bootstrap samples from a signal’s history). The results, shown and explained more precisely in the supplement, are vastly different (worse) than the original set of results. In both forecasting and hotspot prediction, the “fake” indicator models offered essentially no improvement over the pure AR model, which strongly rejects (informally speaking) the implicit regularization hypothesis.

On the topic of regularization, it is also worth noting that the use of ℓ_1 regularization (tuned by cross-validation) in fitting any of the models in (1), (3), (4), or (5) did not generally improve their performance (experiments not shown). This is likely due to the fact that the number of training samples is large compared to the number of features (6,426 training samples and only 3–6 features).

2.3 Evaluation in Up, Down, and Flat Periods

The course of the pandemic has played out quite differently across space and time. Aggregating case rates nationally shows three pronounced waves, but the behavior is more nuanced at the HRR level. Figure 2 is a single example of a forecast in a period of relatively flat case trends, as New York City enters what would become its second wave. The AR forecaster’s 50% prediction interval contains this upswing, but its forecasted median is clearly below the finalized case data. Unfortunately, this behavior is fairly typical of all forecasters: during upswings, the forecasted median tends to fall below the target, while the reverse is true during downswings.

Figure 4 shows histograms of the differences in WIS of the AR model and each indicator model, where we stratify these differences by whether the target occurs during a period of increasing cases rates (up), decreasing case rates (down), or flat case rates (flat). To define the increasing period, we use the same definition we used for the hotspot task in Table 1. Therefore all hotspots are “up”, while all non-hotspots are either “flat” or “down”. For the “down” scenario, we simply use the opposite of the hotspot definition: $Y_{\ell,t}$ decreases by more than 20% relative to the preceding week.

While the performance of all forecasters, including AR, will generally degrade in up periods, different models exhibit different and interesting patterns. CHNG-CLI, CHNG-COVID, Google-AA, and especially CTIS-CLI-in-community have large right tails (displaying improvements over AR) during the down periods. Google-AA and CTIS-CLI-in-community have large right tails during the flat periods. CHNG-CLI and DV-CLI have large left tails (poor forecasts relative to AR) in flat and up periods. Google-AA is the only model that outperforms the AR model, on average, over up periods. Overall, the indicators seem to help more during flat or down periods than up periods, with the exception of Google-AA.

The supplement pursues this analysis further. For example, we examine classification accuracy and log-likelihood for the hotspot task and find a similar phenomenon: the indicators considerably improve accuracy or log-likelihood during flat or down periods, with more mixed behavior during up periods when CHNG-CLI, CHNG-COVID, and DV-CLI, in particular, lead to decreased performance.

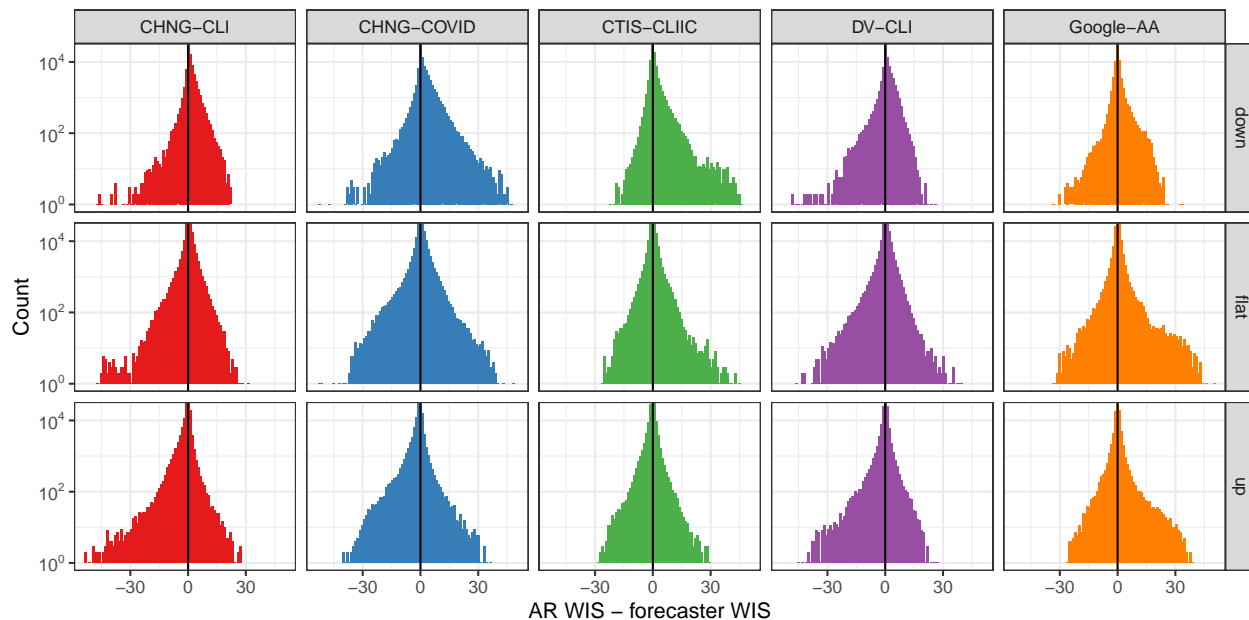


Figure 4: Histogram of the difference in WIS for the AR model and that for each indicator model, stratified by up, down, or flat period, measured in terms of case trends. Note that *larger* differences here are better for each indicator model. The y-axis is on the log scale to emphasize tail behavior.

2.4 Effects of Leading or Lagging Behavior

As described in the methods section, each of the indicators we examine could be said to measure aspects of disease progression that would precede a positive test. That is, we imagine that these signals should “lead” cases. It is entirely reasonable to imagine that, prior to an increase of confirmed COVID-19 tests reported by a public health authority in a particular location, we would see an increase in medical insurance claims for COVID-related outpatient visits. However, it may well be the case that such behavior is different during different periods. In fact, we find empirically that the “leadingness” of an indicator (degree to which it leads case activity) tends to be more pronounced in down or flat periods than in up periods, a plausible explanation for the decreased performance in up periods noted above.

In the supplement, we show how to define a quantitative score to measure the leadingness of an indicator, at any time t and any location ℓ , based on cross correlations to case rates over a short time window around t . The higher this score, the greater it “leads” case activity. Figure 5 displays correlations between the leadingness score of an indicator and the WIS difference (AR model minus an indicator model), stratified by whether the target is classified as up, down, or flat. One would naturally expect that the WIS difference would be positively correlated with leadingness. Somewhat surprisingly, this relationship turns out to be strongest in down periods and weakest in up periods. In fact, it is very nearly the case that for each indicator, the strength of correlations only decreases as we move from down to flat to up periods. In the supplement, we extend this analysis by studying analogous “laggingness” scores, but we do not find as clear patterns.

3 Discussion

Can auxiliary indicators improve COVID-19 forecasting and hotspot prediction models? Our answer, based on analyzing five auxiliary indicators from the COVIDcast API (defined using from medical insurance claims, internet-based surveys, and internet search trends) is undoubtedly “yes”. However, there are levels of nuance to such an answer that must be explained. None of the indicators that we have investigated appear to be the “silver bullet” that one might have hoped for, revolutionizing the tractability of the prediction problem, rendering it easy when it was once hard (in the absence of auxiliary information). Rather, the gains in accuracy from the indicator models (over an autoregressive model based only on past case rates) appear

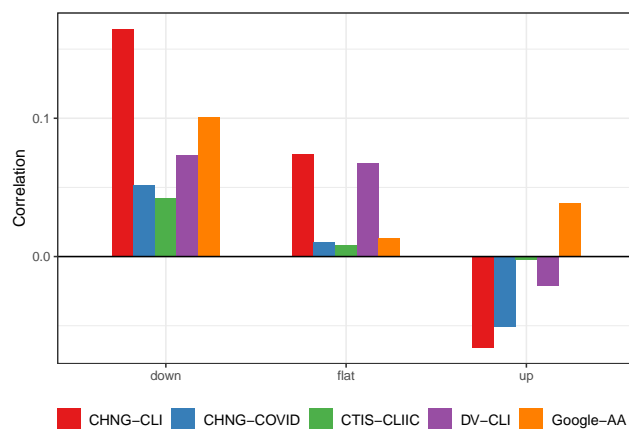


Figure 5: Correlation of the difference in WIS with the “leadingness” of the indicator at the target date, stratified by up, down, or flat period.

to be nontrivial, and consistent across modes of analysis, but modest. In forecasting, the indicator models are found to be most useful in periods in which case rates are flat or trending down, rather than periods in which case rates are trending up (as one might hope to see is the benefit provided by a hypothetical “leading indicator”).

As described previously, it is likely that we could improve the indicator models by using location-specific effects, as well as using nowcasting techniques to estimate finalized indicator values before we use them as features (to account for backfill in the claims-based signals in particular). Beyond this, it is certainly possible that more sophisticated models for forecasting or hotspot prediction would lead to different results, and possibly even different insights. Natural directions to explore include using multiple indicators in a single model, allowing for interaction terms, and leveraging HRR demographics or mobility patterns. That said, we are doubtful that more sophisticated modeling techniques would change the “topline” conclusion—that auxiliary indicators can provide nontrivial, consistent, but modest gains in forecasting and hotspot prediction. Whether a more sophisticated model would be able to leverage the indicators in such a way as to change some of the finer conclusions (e.g., by offering clear improvements in periods in which cases are trending up) is less clear to us.

We reiterate the importance of using vintage data for rigorous backtesting. Data sources that are relevant to public health surveillance are often subject to revision, sometimes regularly (such as medical claims data) and sometimes unpredictably (such as COVID-19 case reports). When analyzing models that are designed to predict future events, if we train these models and make predictions using finalized data, then we are missing a big part of the story. Not only will our sense of accuracy be unrealistic, but certain models may degrade by a greater or lesser extent when they are forced to work with vintage data, so backtesting them with finalized data may lead us to make modeling decisions that are suboptimal for true test-time performance.

In this paper, we have chosen to consider only very simple forecasting models, while devoting most of our effort to accounting for as much of the complexity of the underlying data and evaluation as possible. In fact, our paper is as much about demonstrating how one might address questions about model comparisons and evaluation in forecasting and hotspot prediction in general, as it is about providing rigorous answers to such questions in the context of COVID-19 case rates in particular. We hope that others will leverage our framework, and build on it, so that it can be used to guide work that advances the frontier of predictive modeling for epidemics and pandemics.

Acknowledgements

We thank Matthew Biggerstaff, Logan Brooks, Johannes Bracher, Michael Johansson, Evan Ray, Nicholas Reich, and Roni Rosenfeld for several enlightening conversations about forecasting, scoring, and evaluation. This material is based on work supported by gifts from Facebook, Google.org, the McCune Foundation, and Optum; Centers for Disease Control and Prevention (CDC) grant U01IP001121; the Canadian Statistical Sciences Institute; National Sciences and Engineering Research Council of Canada (NSERC) grant RGPIN-

2021-02618; and National Science Foundation Graduate Research Fellowship Program (NSF GRFP) award DGE1745016.

References

- 1 Delphi Research Group. COVIDcast Epidata API. <https://cmu-delphi.github.io/delphi-epidata/api/covidcast.html>, 2020.
- 2 Delphi Research Group. covidcast: R Client for Delphi's COVIDcast Epidata API. <https://cmu-delphi.github.io/covidcast/covidcastR>, 2020.
- 3 Delphi Research Group. COVIDcast Python API client. <https://cmu-delphi.github.io/covidcast/covidcast-py/html/>, 2020.
- 4 Rob J Hyndman and George Athanasopoulos. *Forecasting: Principles and Practice*. OTexts, 2018.
- 5 Reich Lab. The COVID-19 Forecast Hub. <https://covid19forecasthub.org>, 2020.
- 6 Estee Y Cramer, Evan L Ray, Velma K Lopez, Johannes Bracher, Andrea Brennen, Alvaro J Castro Rivadeneira, Aaron Gerding, Tilmann Gneiting, Katie H House, Yuxin Huang, Dasuni Jayawardena, Abdul H Kanji, Ayush Khandelwal, Khoa Le, Anja Mühlemann, Jarad Niemi, Apurv Shah, Ariane Stark, Yijin Wang, Nutch Wattanachit, Martha W Zorn, Youyang Gu, Sansiddh Jain, Nayana Bannur, Ayush Deva, Mihir Kulkarni, Srujana Merugu, Alpan Raval, Siddhant Shingi, Avtansh Tiwari, Jerome White, Spencer Woody, Maytal Dahan, Spencer Fox, Kelly Gaither, Michael Lachmann, Lauren Ancel Meyers, James G Scott, Mauricio Tec, Ajitesh Srivastava, Glover E George, Jeffrey C Cegan, Ian D Dettwiller, William P England, Matthew W Farthing, Robert H Hunter, Brandon Lafferty, Igor Linkov, Michael L Mayo, Matthew D Parno, Michael A Rowland, Benjamin D Trump, Sabrina M Corsetti, Thomas M Baer, Marisa C Eisenberg, Karl Falb, Yitao Huang, Emily T Martin, Ella McCauley, Robert L Myers, Tom Schwarz, Daniel Sheldon, Graham Casey Gibson, Rose Yu, Liyao Gao, Yian Ma, Dongxia Wu, Xifeng Yan, Xiaoyong Jin, Yu-Xiang Wang, YangQuan Chen, Lihong Guo, Yanting Zhao, Quanquan Gu, Jinghui Chen, Lingxiao Wang, Pan Xu, Weitong Zhang, Difan Zou, Hannah Biegel, Joceline Lega, Timothy L Snyder, Davison D Wilson, Steve McConnell, Robert Walraven, Yunfeng Shi, Xuegang Ban, Qi-Jun Hong, Stanley Kong, James A Turtle, Michal Ben-Nun, Pete Riley, Steven Riley, Ugur Koyluoglu, David DesRoches, Bruce Hamory, Christina Kyriakides, Helen Leis, John Milliken, Michael Moloney, James Morgan, Gokce Ozcan, Chris Schrader, Elizabeth Shakhnovich, Daniel Siegel, Ryan Spatz, Chris Stiefeling, Barrie Wilkinson, Alexander Wong, Zhifeng Gao, Jiang Bian, Wei Cao, Juan Lavista Ferres, Chaozhuo Li, Tie-Yan Liu, Xing Xie, Shun Zhang, Shun Zheng, Alessandro Vespignani, Matteo Chinazzi, Jessica T Davis, Kumpeng Mu, Ana Pastore y Piontti, Xinyue Xiong, Andrew Zheng, Jackie Baek, Vivek Farias, Andreea Georgescu, Retsef Levi, Deeksha Sinha, Joshua Wilde, Nicolas D Penna, Leo A Celi, Saketh Sundar, Sean Cavany, Guido España, Sean Moore, Rachel Oidtman, Alex Perkins, Dave Osthus, Lauren Castro, Geoffrey Fairchild, Isaac Michaud, Dean Karlen, Elizabeth C Lee, Juan Dent, Kyra H Grantz, Joshua Kaminsky, Kathryn Kaminsky, Lindsay T Keegan, Stephen A Lauer, Joseph C Lemaitre, Justin Lessler, Hannah R Meredith, Javier Perez-Saez, Sam Shah, Claire P Smith, Shaun A Truelove, Josh Wills, Matt Kinsey, RF Obrecht, Katharine Tallaksen, John C Burant, Lily Wang, Lei Gao, Zhiling Gu, Myungjin Kim, Xinyi Li, Guannan Wang, Yueying Wang, Shan Yu, Robert C Reiner, Ryan Barber, Emmanuela Gaikedu, Simon Hay, Steve Lim, Chris Murray, David Pigott, B Aditya Prakash, Bijaya Adhikari, Jiaming Cui, Alexander Rodríguez, Anika Tabassum, Jiajia Xie, Pinar Keskinocak, John Asplund, Arden Baxter, Buse Eylul Oruc, Nicoleta Serban, Sercan O Arik, Mike Dusenberry, Arkady Epshteyn, Elli Kanal, Long T Le, Chun-Liang Li, Tomas Pfister, Dario Sava, Rajarishi Sinha, Thomas Tsai, Nate Yoder, Jinsung Yoon, Leyou Zhang, Sam Abbott, Nikos I Bosse, Sebastian Funk, Joel Hellewel, Sophie R Meakin, James D Munday, Katherine Sherratt, Mingyuan Zhou, Rahi Kalantari, Teresa K Yamana, Sen Pei, Jeffrey Shaman, Turgay Ayer, Madeline Adee, Jagpreet Chhatwal, Ozden O Dalgic, Mary A Ladd, Benjamin P Linas, Peter Mueller, Jade Xiao, Michael L Li, Dimitris Bertsimas, Omar Skali Lami, Saksham Soni, Hamza Tazi Bouardi, Yuanjia Wang, Qinxia Wang, Shanghong Xie, Donglin Zeng, Alden Green, Jacob Bien, Addison J Hu, Maria Jahja, Balasubramanian Narasimhan, Samyak Rajanala,

- Aaron Rumack, Noah Simon, Ryan J Tibshirani, Rob Tibshirani, Valerie Ventura, Larry Wasserman, Eamon B O’Dea, John M Drake, Robert Pagano, Jo W Walker, Rachel B Slayton, Michael Johansson, Matthew Biggerstaff, and Nicholas G Reich. Evaluation of individual and ensemble probabilistic forecasts of COVID-19 mortality in the US. medRxiv, 2021.
- 7 Delphi Research Group. evalcast: Tools for Evaluating COVID Forecasters with Proper Data Versioning. <https://cmu-delphi.github.io/covidcast/evalcastR>, 2020.
 - 8 C. W. J. Granger. Investigating causal relations by econometric models and cross-spectral methods. *Econometrica*, 37(3):424–438, 1969.
 - 9 Francis X Diebold and Robert S Mariano. Comparing predictive accuracy. *Journal of Business & Economic Statistics*, 20(1):134–144, 2002.
 - 10 Michael W McCracken. Asymptotics for out of sample tests of Granger causality. *Journal of Econometrics*, 140(2):719–752, 2007.
 - 11 Francis X Diebold. Comparing predictive accuracy, twenty years later: A personal perspective on the use and abuse of diebold–mariano tests. *Journal of Business & Economic Statistics*, 33(1):1–24, 2015.
 - 12 Patrick A. Stokes and Patrick L. Purdon. A study of problems encountered in Granger causality analysis from a neuroscience perspective. *Proceedings of the National Academy of Sciences*, 114(34):E7063–E7072, 2017.
 - 13 Jing Lei, Max G’Sell, Alessandro Rinaldo, Ryan J. Tibshirani, and Larry Wasserman. Distribution-free predictive inference for regression. *Journal of the American Statistical Association*, 113(523):1094–1111, 2018.
 - 14 Alessandro Rinaldo, Ryan J. Tibshirani, and Larry Wasserman. Comment: Statistical inference from a predictive perspective. *Statistical Science*, 34(4):599–603, 2019.
 - 15 Brian D Williamson, Peter B Gilbert, Noah R Simon, and Marco Carone. A unified approach for inference on algorithm-agnostic variable importance. arXiv: 2004.03683, 2020.
 - 16 Lu Zhang and Lucas Janson. Floodgate: Inference for model-free variable importance. arXiv: 2007.01283, 2020.
 - 17 Ben Dai, Xiaotong Shen, and Wei Pan. Significance tests of feature relevance for a blackbox learner. arXiv: 2103.04985, 2021.
 - 18 Daniel Fryer, Inga Strümke, and Hien Nguyen. Shapley values for feature selection: The good, the bad, and the axioms. arXiv: 2102.10936, 2021.
 - 19 Ensheng Dong, Hongru Du, and Lauren Gardner. An interactive web-based dashboard to track COVID-19 in real time. *The Lancet Infectious Diseases*, 20(5):533–534, 2020.
 - 20 Google. COVID-19 search trends symptoms dataset. <http://goo.gle/covid19symptomdataset>, 2020.
 - 21 T. Klopfenstein, N.J. Kadiane-Oussou, L. Toko, P.-Y. Royer, Q. Lepiller, V. Gendrin, and S. Zayet. Features of anosmia in COVID-19. *Médecine et Maladies Infectieuses*, 50(5):436–439, 2020.
 - 22 Luigi A Vaira, Giovanni Salzano, Giovanna Deiana, and Giacomo De Riu. Anosmia and ageusia: Common findings in COVID-19 patients. *The Laryngoscope*, 130:1787, 2020.
 - 23 John E. Wennberg and Megan McAndrew Cooper. *The Dartmouth Atlas of Health Care in the United States*. American Hospital Publishing, Chicago, 1998.
 - 24 Roger Koenker and Gilbert Bassett. Regression quantiles. *Econometrica*, 46(1):33–50, 1978.
 - 25 Roger Koenker. *Quantile Regression*. Cambridge University Press, 2005.

- 26 Roger Koenker and Zhijie Xiao. Quantile autoregression. *Journal of the American Statistical Association*, 101(475):980–990, 2006.
- 27 Tilmann Gneiting and Adrian E Raftery. Strictly proper scoring rules, prediction, and estimation. *Journal of the American Statistical Association*, 102(477):359–378, 2007.
- 28 Johannes Bracher, Evan L. Ray, Tilmann Gneiting, and Nicholas G Reich. Evaluating epidemic forecasts in an interval format. *PLOS Computational Biology*, 17(2):1–15, 2021.
- 29 Shailesh Bavadekar, Andrew Dai, John Davis, Damien Desfontaines, Ilya Eckstein, Katie Everett, Alex Fabrikant, Gerardo Flores, Evgeniy Gabrilovich, Krishna Gadepalli, Shane Glass, Rayman Huang, Chaitanya Kamath, Dennis Kraft, Akim Kumok, Hinali Marfatia, Yael Mayer, Benjamin Miller, Adam Pearce, Irippuge Milinda Perera, Venky Ramachandran, Karthik Raman, Thomas Roessler, Izhak Shafran, Tomer Shekel, Charlotte Stanton, Jacob Stimes, Mimi Sun, Gregory Wellenius, , and Masrour Zoghi. Google COVID-19 search trends symptoms dataset: Anonymization process description. arXiv: 2009.01265, 2020.

Supplemental information

A Examining the relative advantage of using finalized rather than vintage data

The goal of this section is to quantify the effect of not properly accounting for the question of “what was known when” in performing retrospective evaluations of forecasters. Figures 6 and 7 show what Figures 3 and 4 in the main paper would have looked like if we had simply trained all models using the finalized data rather than using vintage data. This comparison can be seen more straightforwardly in Figures 8 and 9, which show the ratio in performance between the vintage and finalized versions. When methods are given the finalized version of the data rather than the version available at the time that the forecast would have been made, all methods appear (misleadingly) to have better performance than they would have had if run prospectively. For example, for forecasting case rates 7-days ahead, the WIS of all methods is at least 8% larger than what would have been achieved using finalized data. This effect diminishes as the forecasting horizon increases, reflecting the fact that longer-horizon forecasters rely less heavily on recent data than very short-horizon forecasters. Crucially, some methods are “helped” more than others by the less scrupulous retrospective evaluation, underscoring the difficulty of avoiding misleading conclusions when performing retrospective evaluations of forecasters.

CHNG-CLI (and, to a lesser extent, the other claims-based signals) is the most affected by this distinction, reflecting the latency in claims-based reporting. This underscores the importance of efforts to provide “nowcasts” for claims signals (which corresponds to a 0-ahead forecast of what the claims signal’s value will be once all data has been collected). Looking at the CHNG-CLI and DV-CLI curves in Figure 6, we can see that they perform very similarly when trained on the finalized data. This is reassuring because they are, in principle, measuring the same thing (namely, the percentage of outpatient visits that are primarily about COVID-related symptoms). The substantial difference in their curves in Figure 3 of the main paper must therefore reflect their having very different backfill profiles.

While using finalized rather than vintage data affects DV-CLI the least for forecasting, it is one of the most affected methods for the hotspot problem. This is a reminder that the forecasting and hotspot problems are fundamentally distinct. For example, the hotspot problem does not measure the ability to distinguish between flat and downward trends.

Even the AR model is affected by this distinction, reflecting the fact that the case rates themselves (i.e., the response values) are also subject to revision. The forecasters based on indicators are thus affected both by revisions to the indicators and by revisions to the case rates. In the case of the Google-AA model, in which we only used finalized values for the Google-AA indicator, the difference in performance can be wholly attributed to revisions of case rates.

B Aggregating with geometric mean

In this section, we consider using the geometric mean instead of the arithmetic mean when aggregating the weighted interval score (WIS) across location-time pairs. There are three reasons why using the geometric mean may be desirable.

1. WIS is right-skewed, being bounded below by zero and having occasional very large values. Figure 10 illustrates that the densities appear roughly log-Gaussian. The geometric mean is a natural choice in such a context since the relative ordering of forecasters is determined by the arithmetic mean of the *logarithm* of their WIS values.
2. In the main paper, we report the ratio of the mean WIS of a forecaster to the mean WIS of the baseline forecaster. Another choice could be to take the mean of the ratio of WIS values for the two methods. This latter choice would penalize a method less for doing poorly where the baseline forecaster also does poorly. Using instead the geometric mean makes the order of aggregation and scaling immaterial since the ratio of geometric means is the same as the geometric mean of ratios.

3. If one imagines that a forecaster’s WIS is composed of multiplicative space-time effects $S_{\ell,t}$ shared across all forecasters, i.e. $\text{WIS}(F_{\ell,t,f}, Y_{\ell,t}) = S_{\ell,t} E_{f,t}$ with $E_{f,t}$ a forecaster-specific error, then taking the ratio of two forecasters’ geometric mean WIS values will effectively cancel these space-time effects.

Figure 11 uses the geometric mean for aggregation. Comparing this with Figure 3 of the main paper, we see that the main conclusions are largely unchanged; however, CHNG-CLI now appears better than AR. This behavior would be expected if CHNG-CLI’s poor performance is attributable to a relatively small number of large errors (as opposed to a large number of moderate errors). Indeed, Figure 5 of the main paper further corroborates this, in which we see the heaviest left tails occurring for CHNG-CLI.

C Bootstrap results

As explained in Section 2.B. of the main paper, a (somewhat cynical) hypothesis for why we see benefits in forecasting and hotspot prediction is that the indicators are not actually providing useful information but they are instead acting as a sort of “implicit regularization,” leading to shrinkage on the autoregressive coefficients and therefore to less volatile predictions. To investigate this hypothesis, we consider fitting “noise features” that in truth should have zero coefficients. Recall (from the main paper) that at each forecast date, we train a model on 6,426 location-time pairs. Indicator models are based on six features, corresponding to the three autoregressive terms and the three lagged indicator values. To form noise indicator features, we replace their values with those from a randomly chosen time-space pair (while keeping the autoregressive features fixed). In particular, at each location ℓ and time t , for the forecasting task we replace the triplet $(X_{\ell,t}, X_{\ell,t-7}, X_{\ell,t-14})$ in Eq. (3) of the main paper with the triplet $(X_{\ell^*,t^*}, X_{\ell^*,t^*-7}, X_{\ell^*,t^*-14})$, where (ℓ^*, t^*) is a location-time pair sampled with replacement from the 6,426 location-time pairs. Likewise in the hotspot prediction task, we replace the triplet $(X_{\ell,t}^\Delta, X_{\ell,t-7}^\Delta, X_{\ell,t-14}^\Delta)$ in Eq. (5) of the main paper with $(X_{\ell^*,t^*}^\Delta, X_{\ell^*,t^*-7}^\Delta, X_{\ell^*,t^*-14}^\Delta)$. Figures 12–14 show the results. No method exhibits a noticeable performance gain over the AR method, leading us to dismiss the implicit regularization hypothesis.

D Upswings and Downswings

In this section we provide extra details about the upswing / flat / downswing analysis described in the main text. Figure 15 shows the overall results, examining the average difference $\text{WIS}(AR) - \text{WIS}(F)$ in period. Figure 16 shows the same information for the hotspot task. On average, during downswings and flat periods, the indicator-assisted models have lower classification error and higher log likelihood than the AR model. For hotspots, both Google-AA and CTIS-CLIIC perform better than the AR model during upswings, in contrast to the forecasting task, where only Google-AA improves. For a related analysis, Figure 17 shows histograms of the Spearman correlation (Spearman’s ρ , a rank-based measure of association) between the $\text{WIS}(F)/\text{WIS}(AR)$ and the magnitude of the swing. Again we see that case rate increases are positively related to diminished performance of the indicator models.

One hypothesis for diminished relative performance during upswings is that the AR model tends to overpredict downswings and underpredict upswings. Adding indicators appears to help avoid this behavior on the downswing but not as much on upswings. Figure 18 shows the correlation between between $\text{WIS}(AR) - \text{WIS}(F)$ and the difference of their median forecasts. During downswings, this correlation is large, implying that improved relative performance of F is related to making lower forecasts than the AR model. The opposite is true during upswings. This is largely to be expected. However, the relationship attenuates in flat periods and during upswings. That is, when performance is better in those cases, it may be due to other factors than simply making predictions in the correct direction, for example, narrower confidence intervals.

E Leadingness and laggingness

In Section 2.D of the main text, we discuss the extent to which the indicators are leading or lagging case rates during different periods. To define the amount of leadingness or laggingness at location ℓ , we use the cross correlation function (CCF) between the two time series. The $\text{CCF}_\ell(a)$ of an indicator X_ℓ and case rates Y_ℓ is defined as their Pearson correlation where X_ℓ has been aligned with the values of Y_ℓ that occurred a days

earlier. Thus, for any $a > 0$, $\text{CCF}_\ell(a) > 0$ indicates that $Y_{\ell,t}$ is moving together with $X_{\ell,t+a}$. In this case we say that X_ℓ is lagging Y_ℓ . For $a < 0$, $\text{CCF}_\ell(a) > 0$ means that $Y_{\ell,t}$ is positively correlated with $X_{\ell,t-a}$, so we say that X_ℓ leads Y_ℓ .

Figure 19 shows the standardized signals for the HRR containing Charlotte, North Carolina, from August 1, 2020 until the end of September. These are the same signals shown in Figure 1 in the manuscript but using finalized data. To define “leadingness” we compute $\text{CCF}_\ell(a)$ (as implemented with the R function `ccf()`) for each $a \in \{-15, \dots, 15\}$ using the 56 days leading up to the target date. This is the same amount of data used to train the forecasters: 21 days of training data, 21 days to get the response at $a = 21$, and 14 days for the longest lagged value. The orange dashed horizontal line represents the 95% significance threshold for correlations based on 56 observations. Any correlations larger in magnitude than this value are considered statistically significant under the null hypothesis of no relationship. We define leadingness to be the sum of the significant correlations that are leading (those above the dashed line with $a < 0$) while laggingness is the same but for $a > 0$. In the figure, there are three significant correlations on the “leading” side (at $a = -5, -4, -3$), so leadingness will be the sum of those values while laggingness is 0: on September 28 in Charlotte, DV-CLI is leading cases leading but not lagging.

Figure 20 shows the correlation between laggingness and the difference in indicator WIS and AR WIS. Unlike leadingness (Figure 5 in the manuscript) there is no obvious relationship that holds consistently across indicators. This is heartening as laggingness should not aid forecasting performance. On the other hand, if an indicator is more lagging than it is leading, this may suggest diminished performance. Figure 21 shows the correlation of the difference in leadingness and laggingness with the difference in WIS. The pattern here is largely similar to the pattern in leadingness described in the manuscript: the relationship is strongest in down periods and weakest in up periods with the strength diminishing as we move from down to flat to up for all indicators.

In calculating the CCF and the associated leadingness and laggingness scores, we have used the finalized data, and we look at the behavior at the target date of the forecast. That is we are using the same data to evaluate predictive accuracy as to determine leadingness and laggingness. It should be noted that the leadingness of the indicator at the time the model is trained may also be important. Thus, we could calculate separate leadingness and laggingness scores for the trained model and for the evaluation data and examine their combination in some way. We do not pursue this combination further and leave this investigation for future work.

F Examining data in 2021

In this section, we investigate the sensitivity of the results to the period over which we train and evaluate the models. In the main paper, we end all evaluation on December 31, 2020. Figures 22–24 show how the results would differ if we extended this analysis through March 31, 2021. Comparing Figure 22 to Figure 3 of the main paper, one sees that as ahead increases most methods now improve relative to the baseline forecaster. When compared to other methods, CHNG-CLI appears much better than it had previously; however, all forecasters other than CHNG-COVID and DV-CLI are performing less well relative to the baseline than before. These changes are likely due to the differing nature of the pandemic in 2021, with flat and downward trends much more common than upward trajectories. Indeed, the nature of the hotspot prediction problem is quite different in this period. With a 21-day training window, it is common for there to be many fewer hotspots in training.

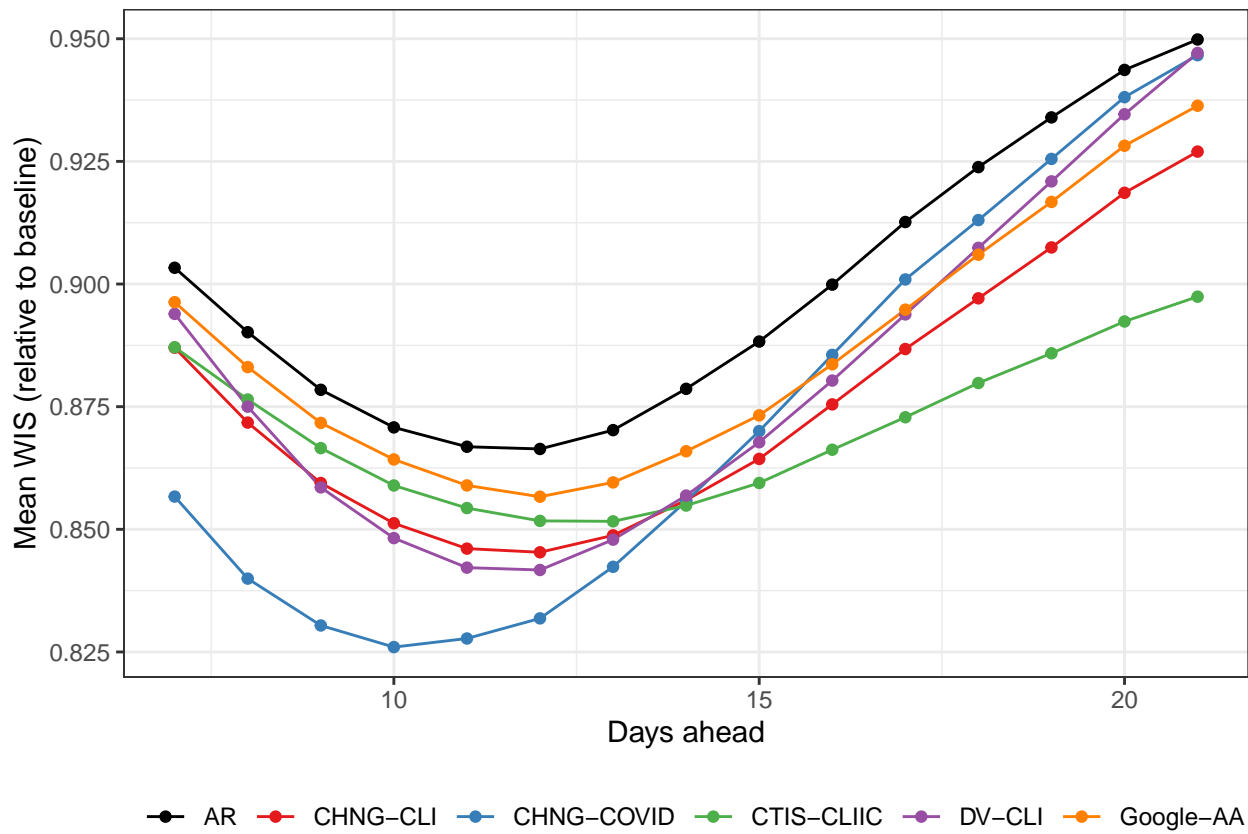


Figure 6: Forecasting performance using finalized data. Compare to Figure 3 in the manuscript.

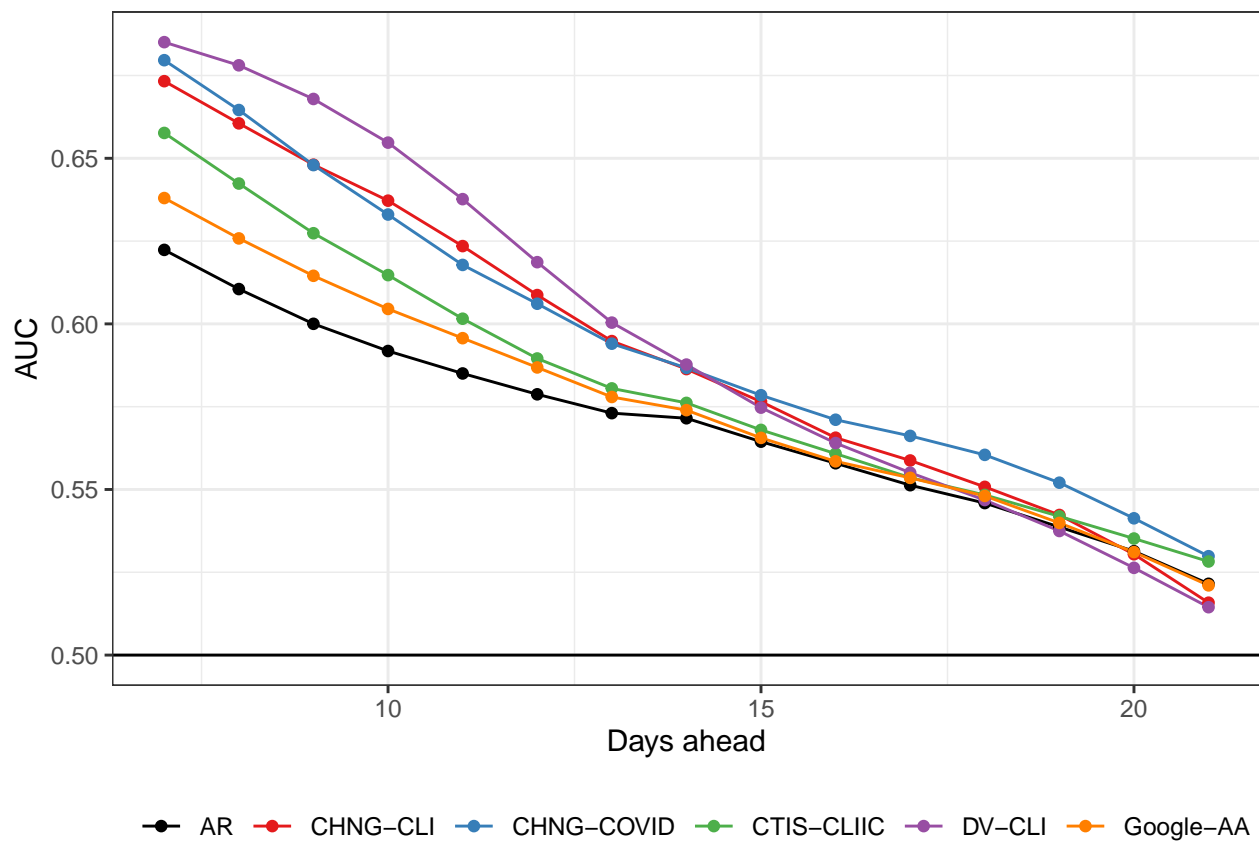


Figure 7: Hotspot prediction performance using finalized data. Compare to Figure 4 in the manuscript.

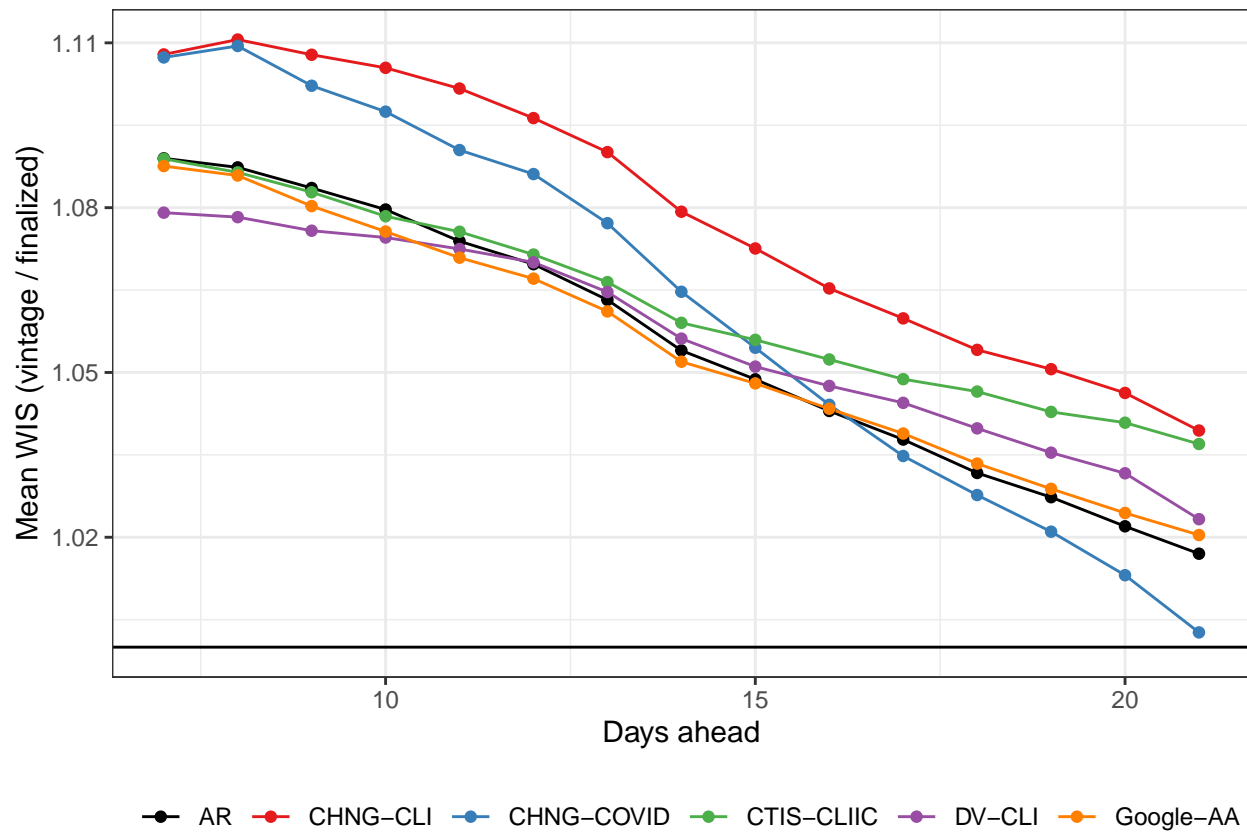


Figure 8: Relative forecast WIS with vintage compared to finalized data. Using finalized data leads to overly optimistic performance.

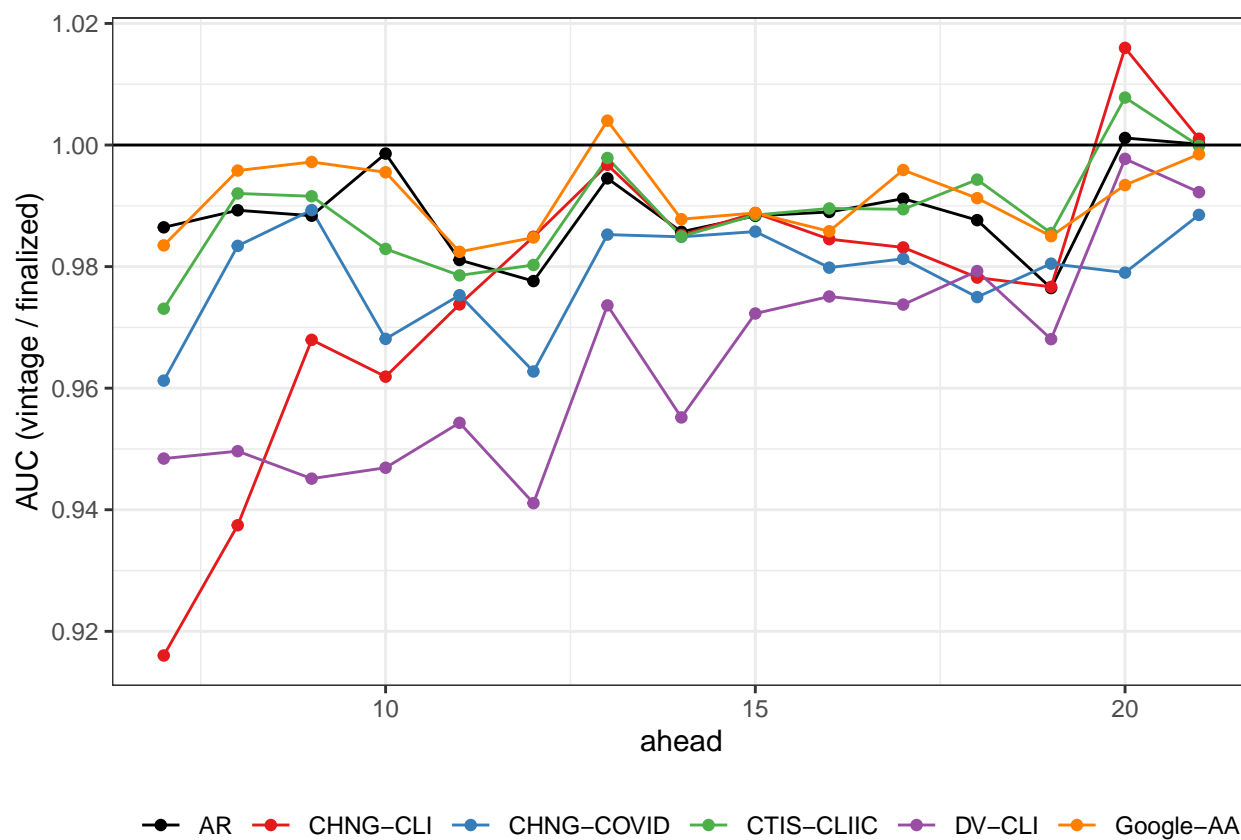


Figure 9: Relative AUC with vintage compared to finalized data. Using finalized data leads to overly optimistic hotspot performance.

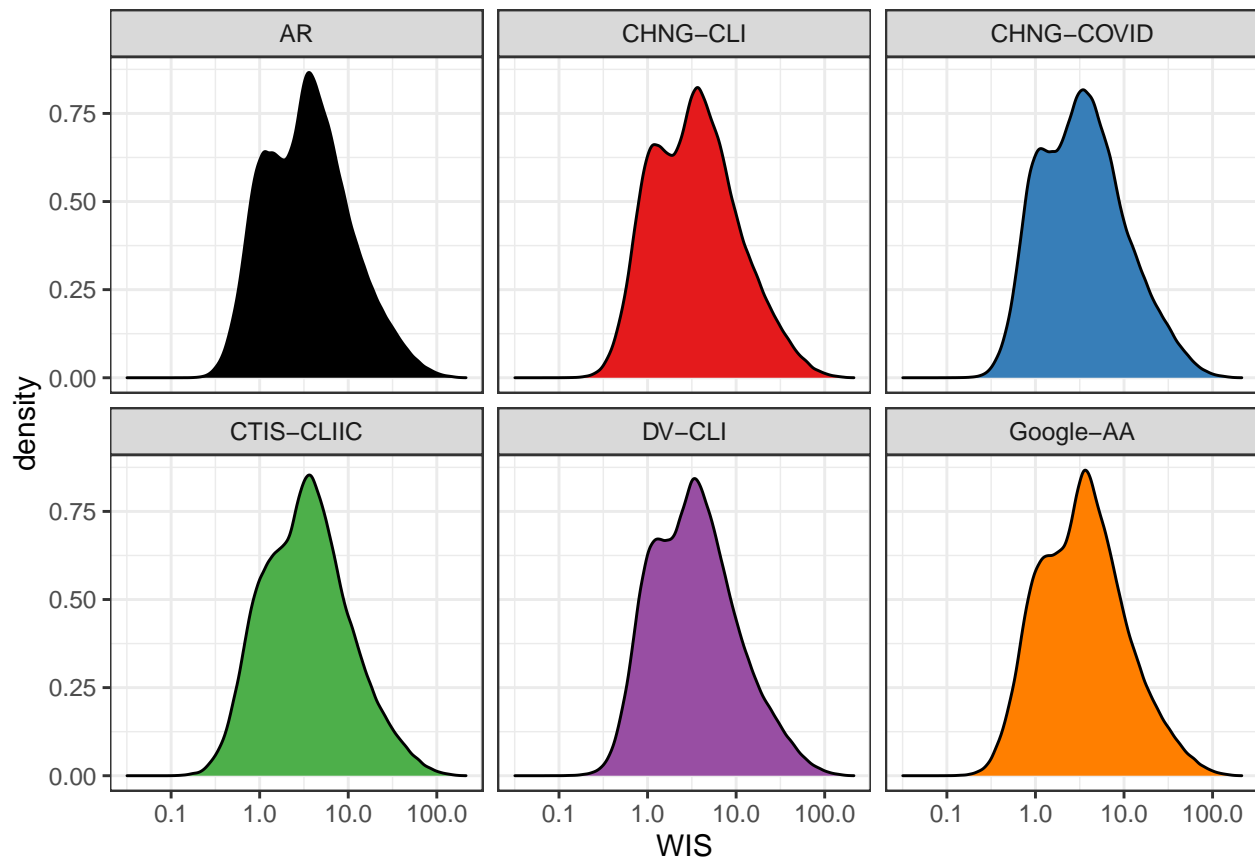


Figure 10: Weighted interval score appears to more closely resemble a log-Gaussian distribution.

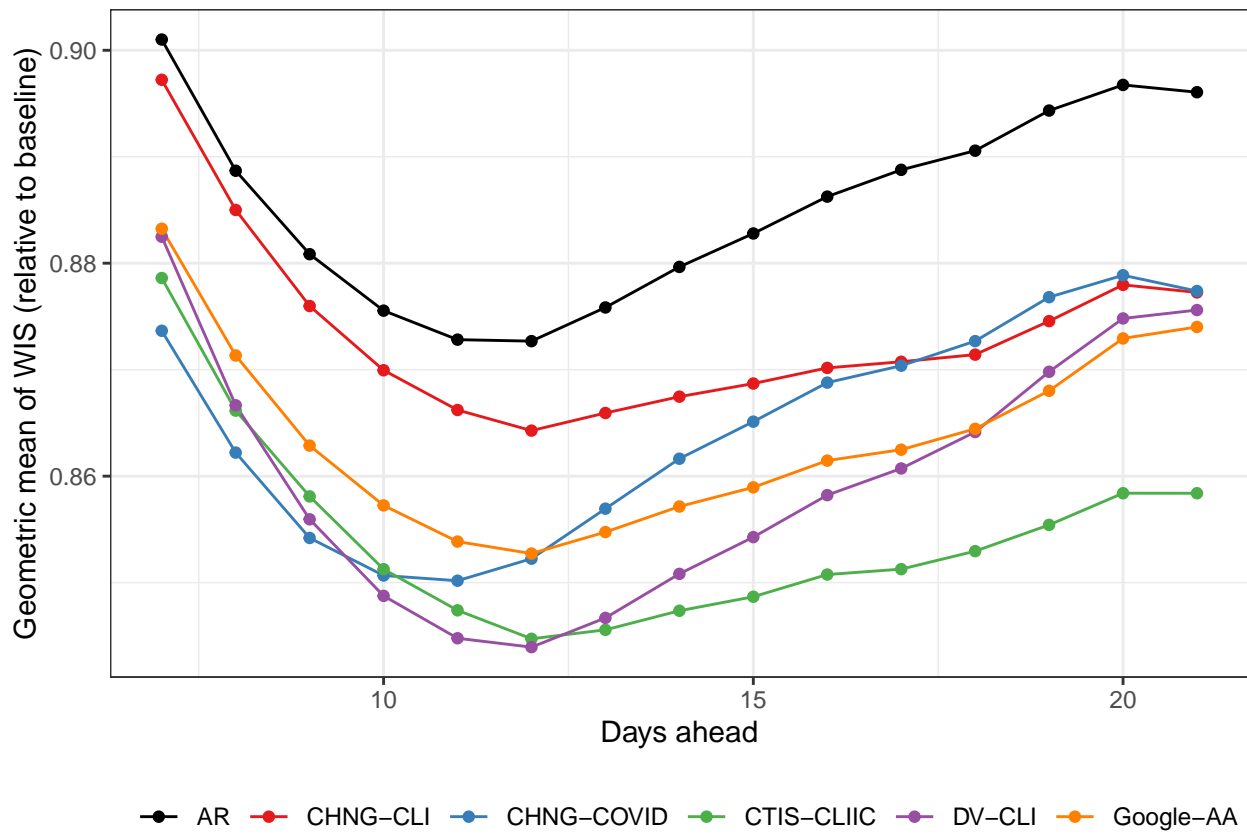


Figure 11: Relative forecast performance using vintage data and summarizing with the more robust geometric mean.

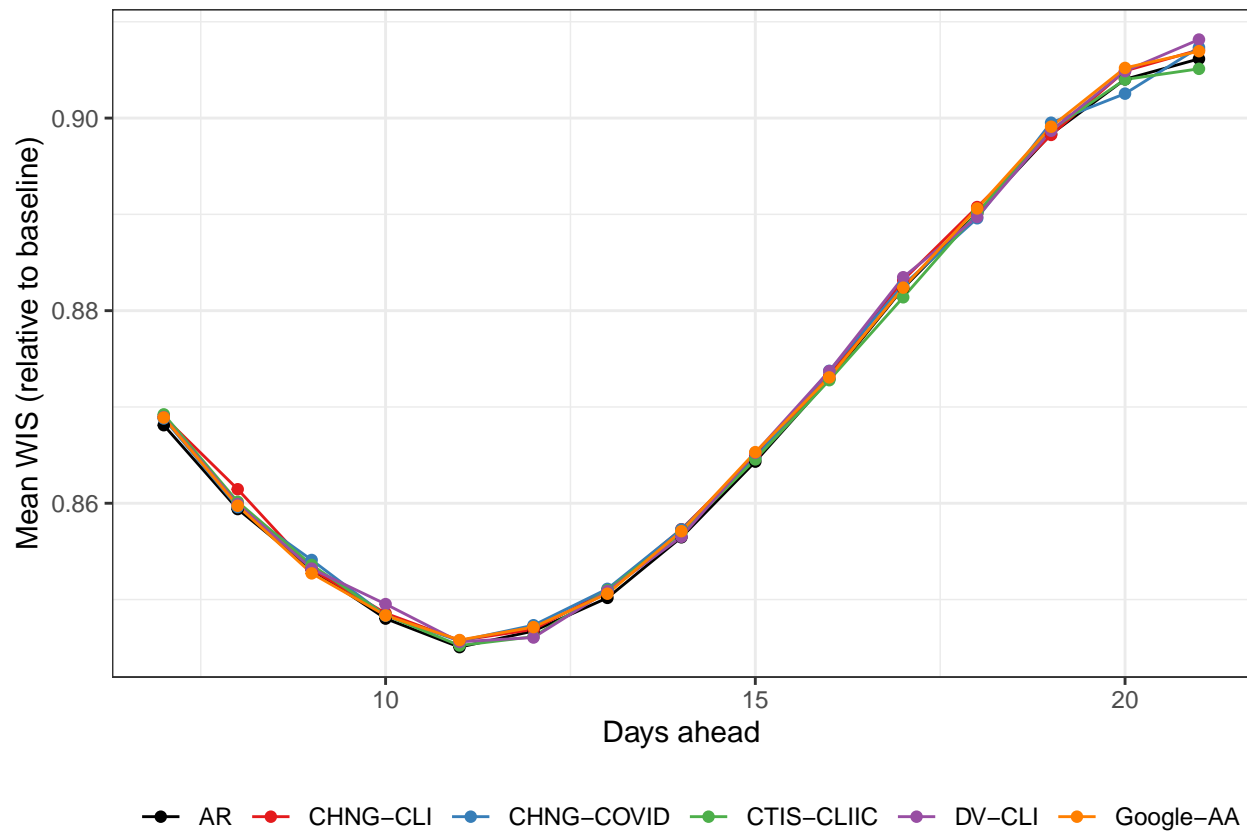


Figure 12: Forecast performance when indicators are replaced with samples from their empirical distribution. Performance is largely similar to the AR model.

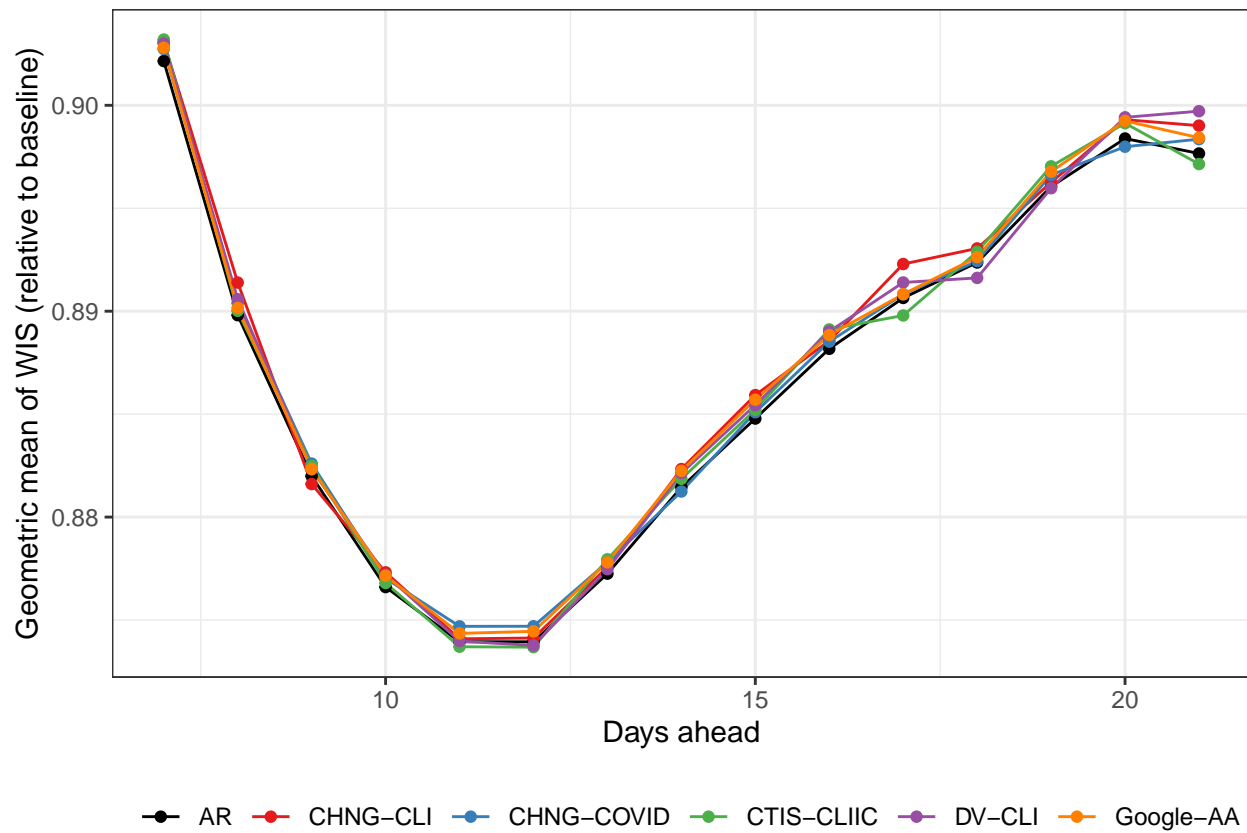


Figure 13: Forecast performance as measured with the geometric mean when indicators are replaced with samples from their empirical distribution. Performance is largely similar to the AR model.

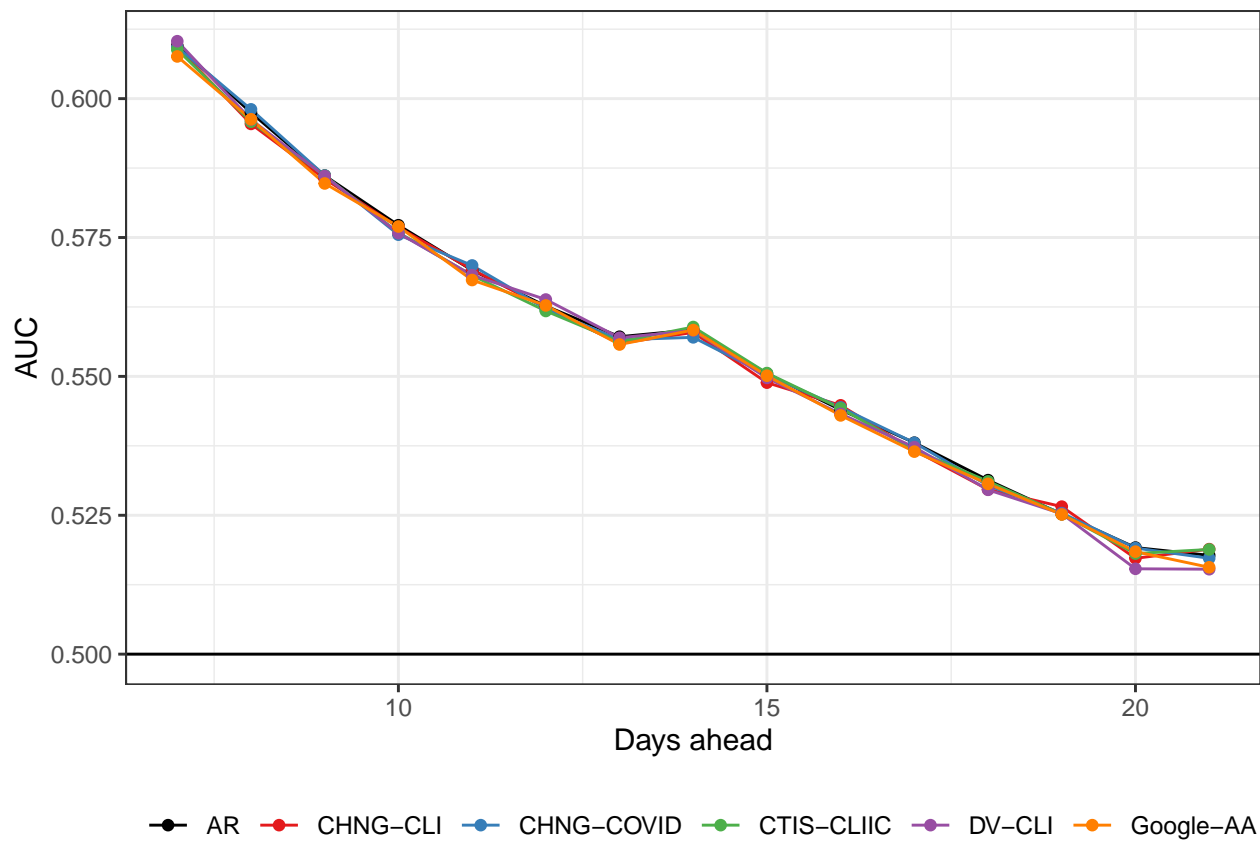


Figure 14: Hotspot prediction performance when indicators are replaced with samples from their empirical distribution. Performance is largely similar to the AR model.

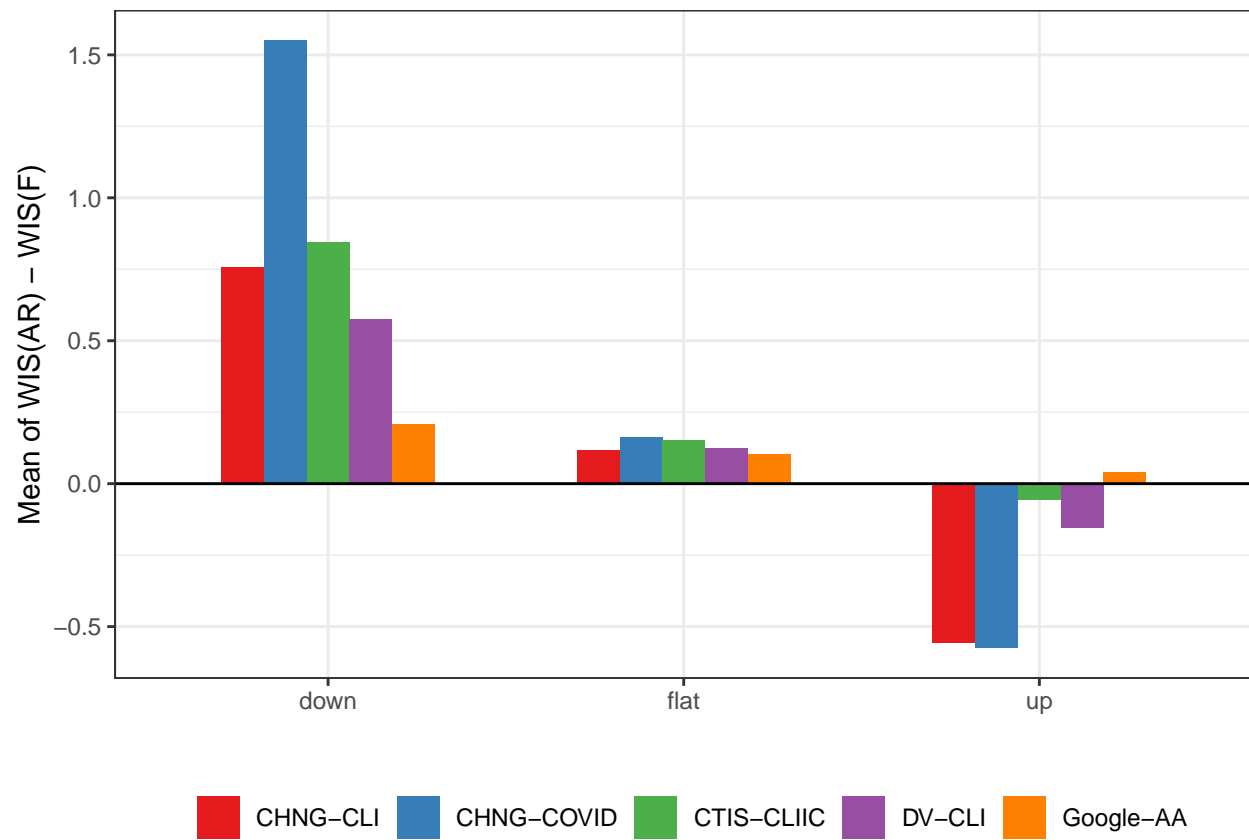


Figure 15: Average difference between the WIS of the AR model and the WIS of the other forecasters. The indicator-assisted forecasters do best during down and flat periods.

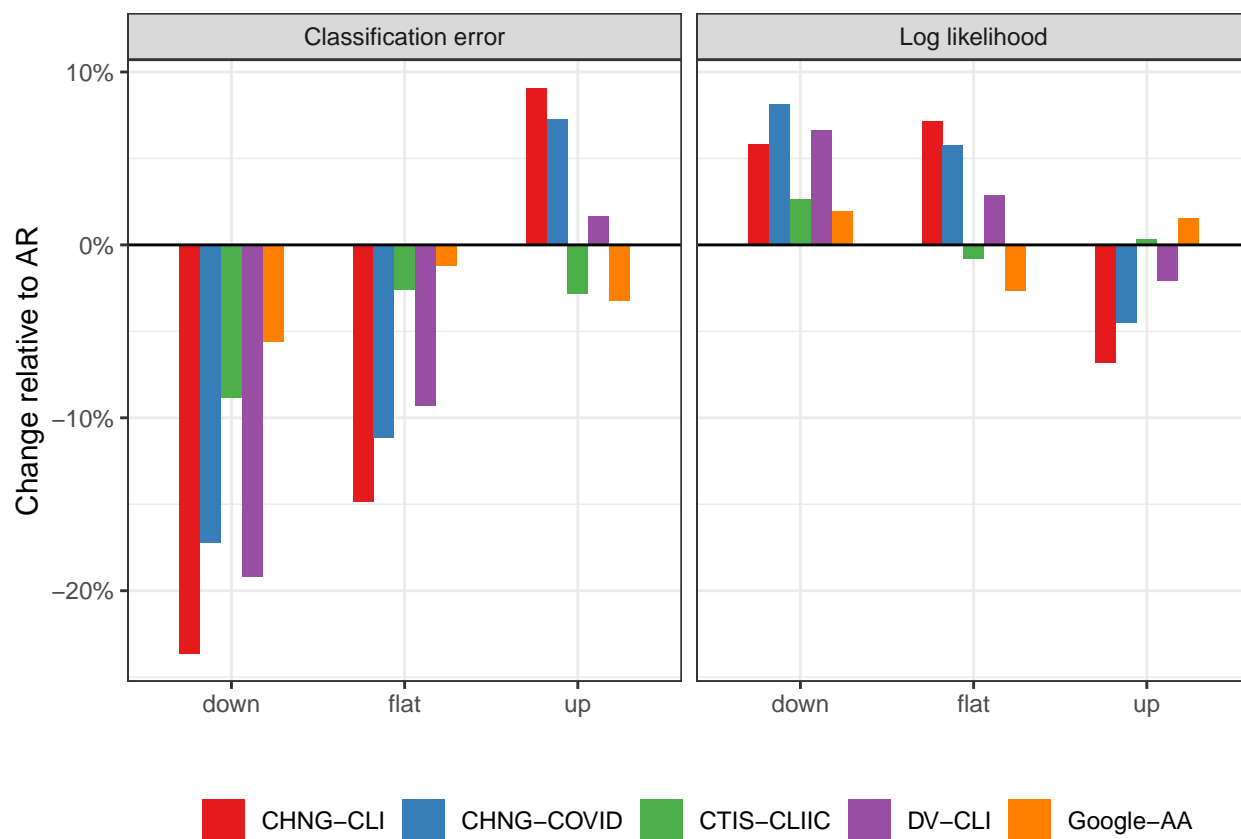


Figure 16: Classification and loglikelihood separated into periods of upswing, downswing, and flat cases. Like the analysis of the forecasting task in the main paper (see Figure 7), performance is better during down and flat periods.

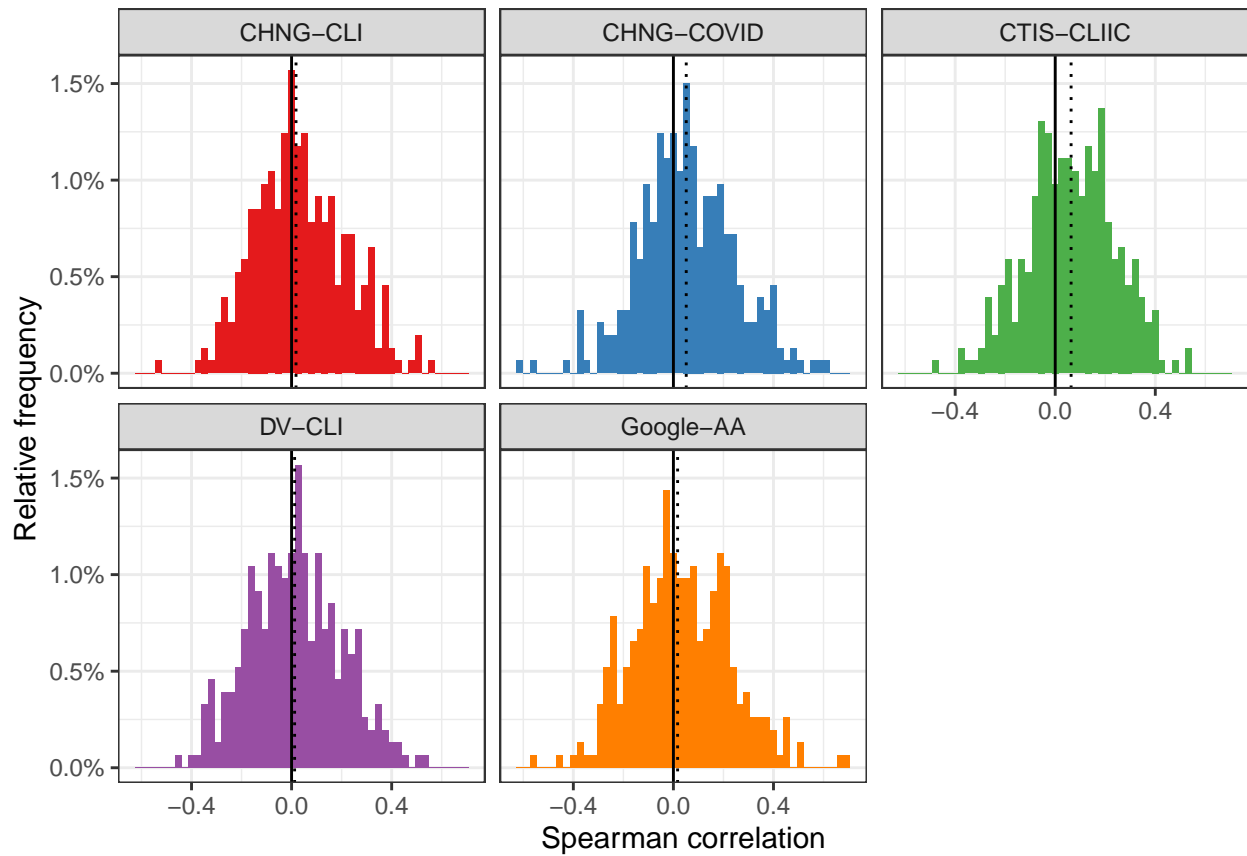


Figure 17: Histograms of the Spearman correlation between the ratio of AR to AR WIS with the percent change in smoothed case rates relative to 7 days earlier.

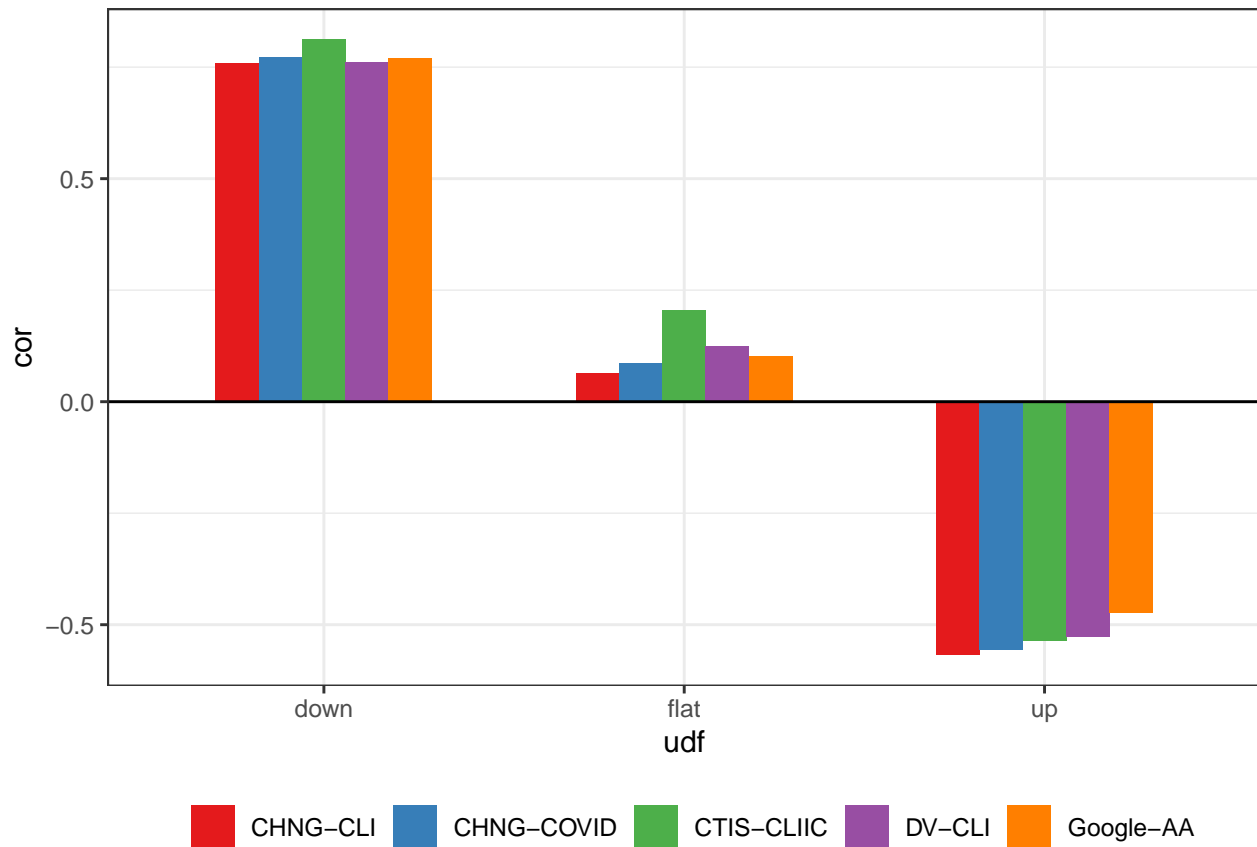


Figure 18: Correlation of the difference in WIS with the difference in median predictions for the AR model relative to the indicator-assisted forecaster. In down periods, improvements in forecast risk are highly correlated with lower median predictions. The opposite is true in up periods. This suggests, as one might expect that improved performance of the indicator-assisted model is attributable to being closer to the truth than the AR model. This conclusion is stronger in down periods than in up periods.

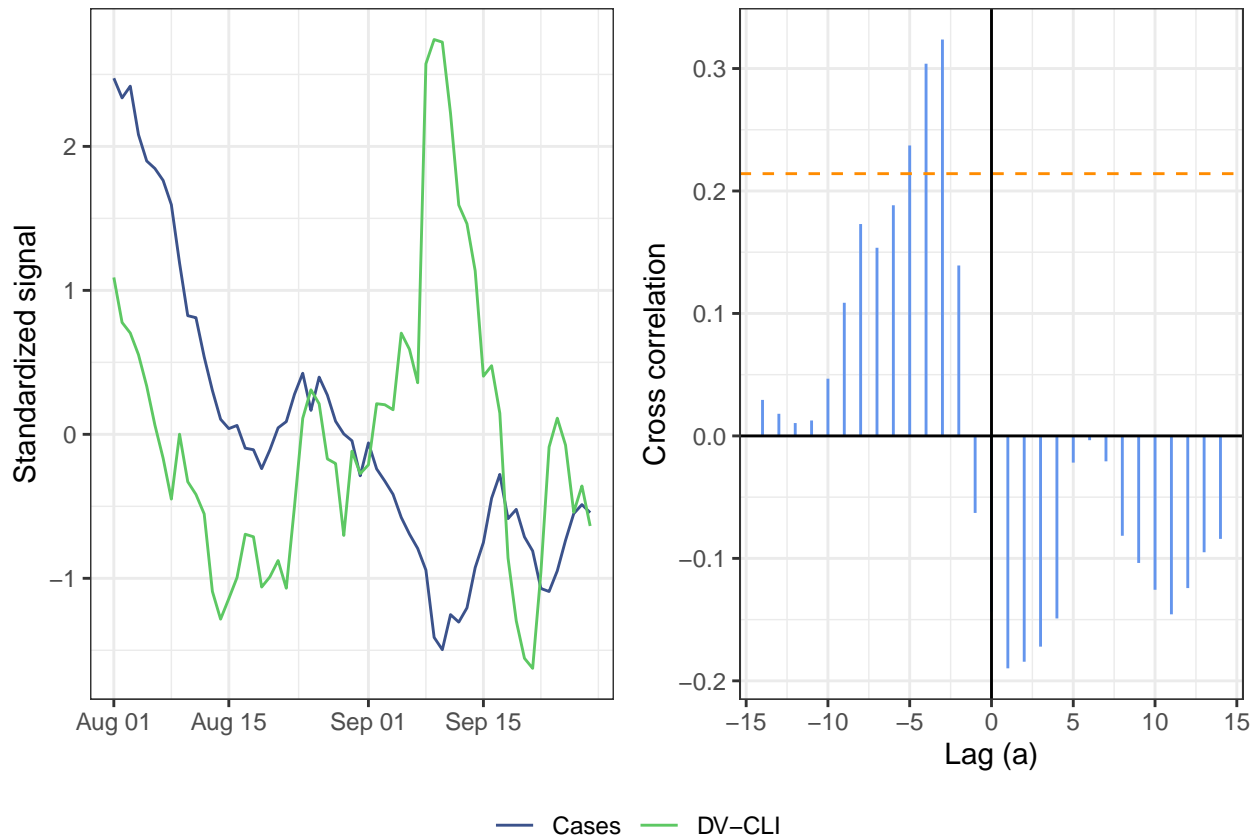


Figure 19: Illustration of the cross-correlation function between DV-CLI and cases. The left panel shows the standardized signals over the period from August 1 to September 28 (as of May 15, 2021). The right panel shows $CCF_{\ell}(a)$ for different values of a as vertical blue bars. The orange dashed lines indicate the 95% significance threshold. By our leadingness/laggingness metric, DV-CLI is leading (but notlagging) cases over this period.

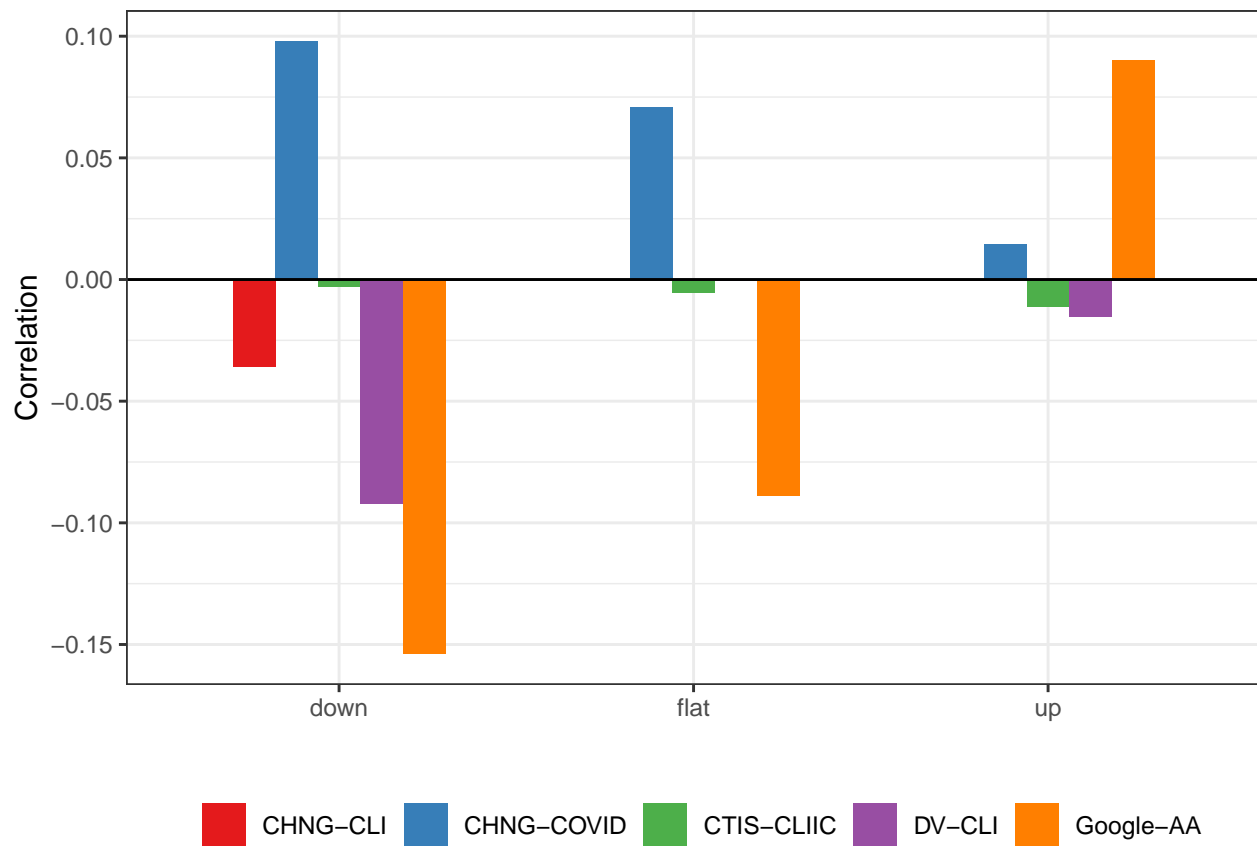


Figure 20: Correlation of the difference in WIS with the laggingness of the indicator at the target date, stratified by up, down, or flat period. Compare to Figure 5 in the manuscript.

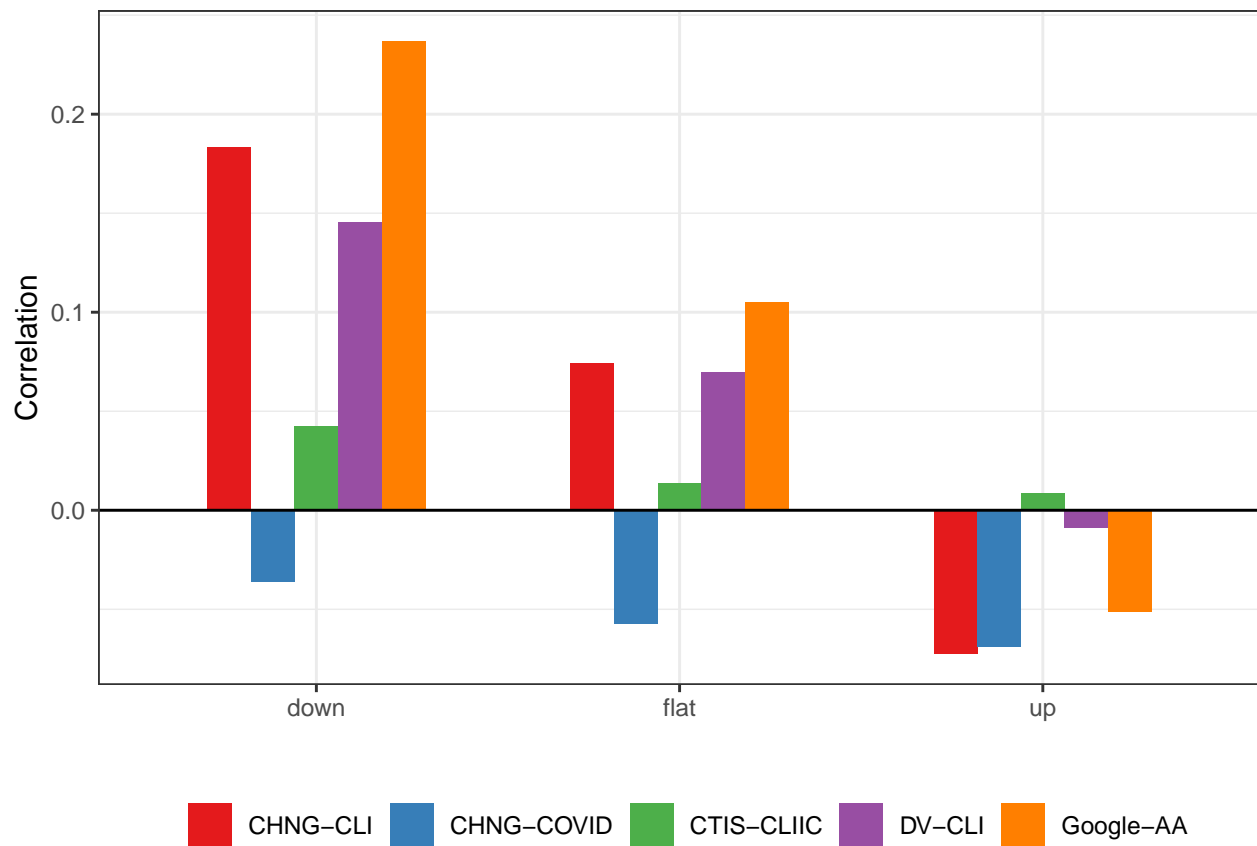


Figure 21: Correlation of the difference between leadingness and laggingness with the difference in WIS. The relationship is essentially the same as described in the manuscript and shown in Figure 5.

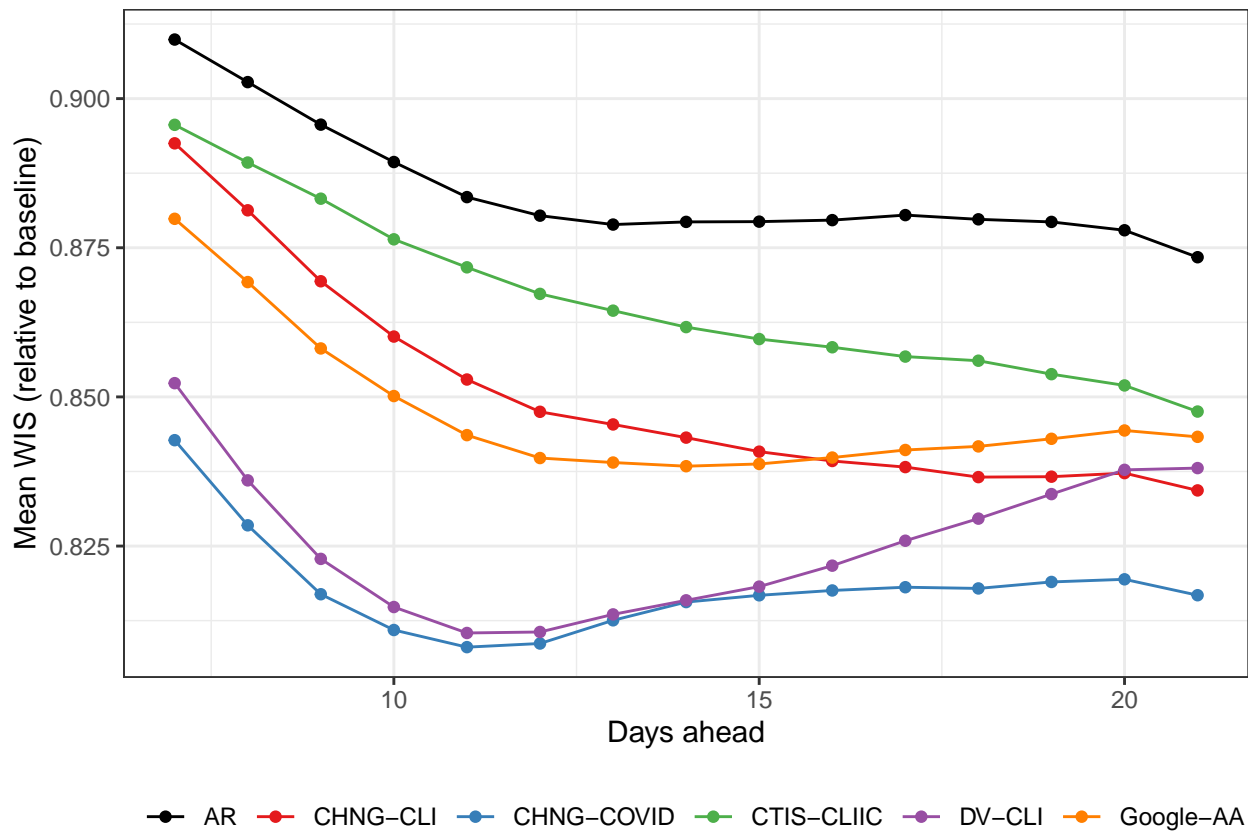


Figure 22: Forecast performance over all periods. Performance largely improves for all forecasters with the inclusion of data in 2021.

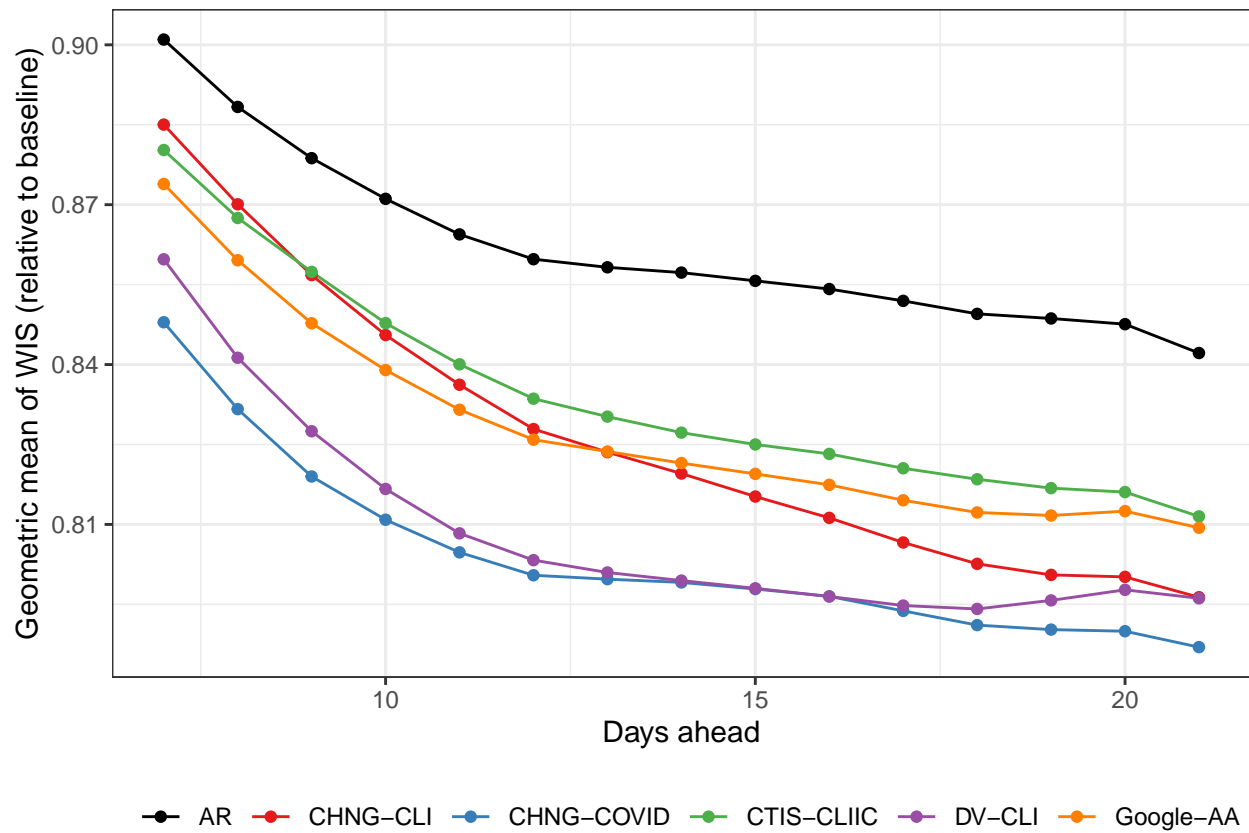


Figure 23: Forecast performance over all periods aggregated with the geometric mean. Again, the inclusion of data in 2021 leads to improved performance.

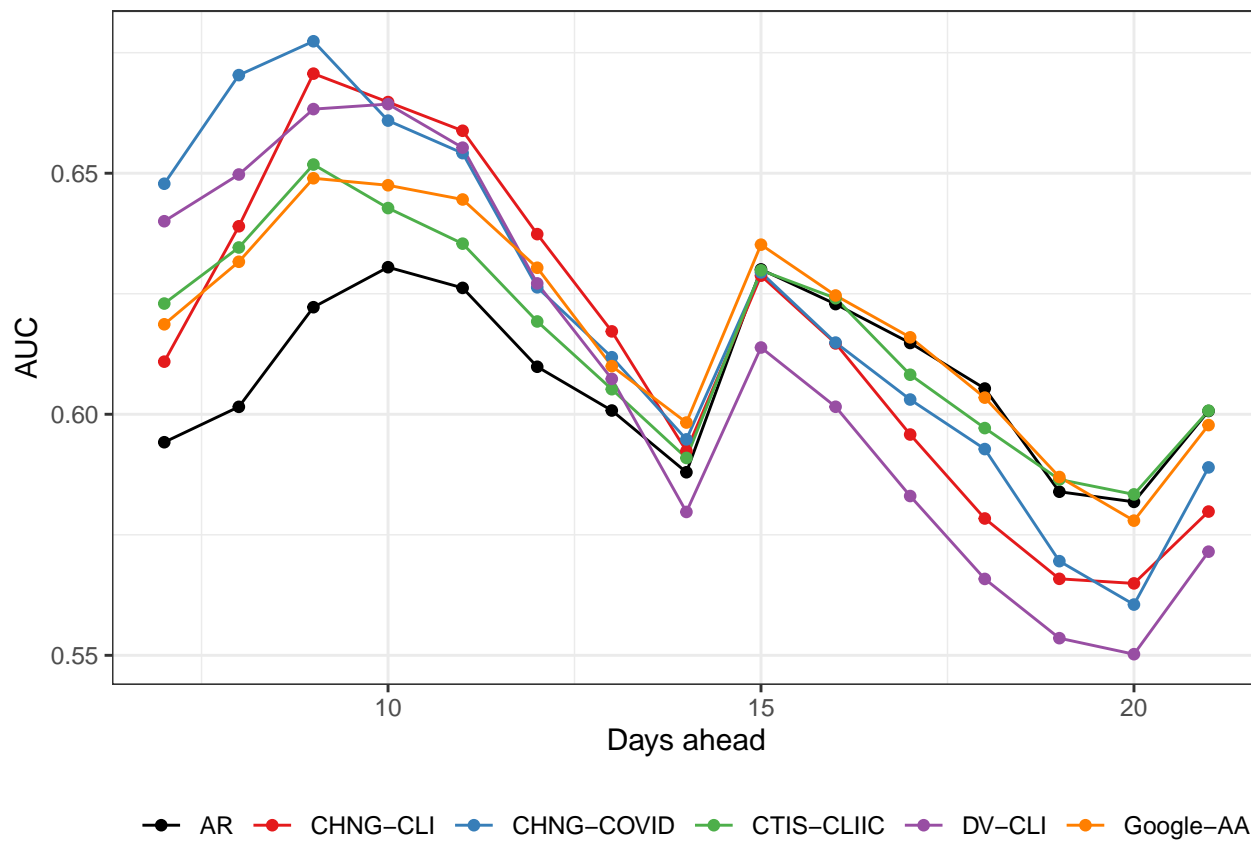


Figure 24: Area under the curve for hotspot predictions including data in 2021. Performance degrades relative to the period in 2020. However, there are far fewer hotspots during this period as case rates declined in much of the country.